

CLASSIFIED OBSERVATION OF SMALL CURRENT INTERRUPTION PHENOMENA IN POWER SYSTEMS

YUKIO KITO

Department of Electrical Engineering

(Received September 30, 1962)

CONTENTS

Introduction

Chapter 1. A Short Review on Switching Phenomena

Chapter 2. Interruption of Line Charging Current at Transformer Terminals with Isolated Neutral

§ 1. Experimental results

- (1.1) Classification of actual reignition phenomena
- (1.2) Phase angles when an arc in each line is easily quenched
- (1.3) Observed sequences of reignitions
- (1.4) Arc duration time and circuit characteristics

§ 2. Theoretical investigations on reignition phenomena

§ 3. Theoretical investigations on overvoltages accompanied with reignitions

- (3.1) Initial reignition
- (3.2) Determination of possible reignitions
- (3.3) Reignition over two or three lines
- (3.4) Line-to-line overvoltages
- (3.5) Original equations

Chapter 3. Interruption of Small Inductive Current with Current Chopping

§ 1. Current interruption of unloaded transformers

§ 2. Overvoltages and "off-peak current ratio"

§ 3. Overvoltages and "prospective charge" to be interrupted

§ 4. Analysed wave forms of three phase inrush current

§ 5. Theoretical determination of possible overvoltage distribution

- (5.1) Determination of prospective charge
- (5.2) Overvoltage estimation by the conception of prospective charge
- (5.3) Results estimated
- (5.4) Supplementary note

Chapter 4. A Few Comments on Switching Surges

§ 1. Standard surges for testing insulations

§ 2. Tolerable reignitions of circuit breakers

§ 3. Overvoltages amended by circuit breaker characteristics

Conclusion

Acknowledgement

References

Introduction

The electrical power system, which recently supplies a great part of energy demand, acquires a deeper significance not only in the extra-high voltage system but in lower voltage ones. The reliability of various apparatus in whole system is raised more and more as they are newly constructed, while circuit breakers tend to take a destructive situation in the systems. They are obliged to give more or less unfavourable influences on the system at every switching operation which is inevitably increased in number to keep better services. Interruption phenomena are always accompanied with electric arcs and their extinction or reignition gives rise to discontinuous variations of physical amounts, which, in turn, result in various kinds of transient phenomena according to system characteristics. Such switching phenomena should be defined by the delicate combination of following three factors; arc, chance of switching and system construction. Many publications have treated overvoltages in these cases under worst conditions provided a priori, or have showed statistical results of the experiments carried out in certain conditions. According to those studies, the severities of switching surges are either overestimated or underestimated, and the testing of insulations in various apparatus is not carried out by suitable wave forms for switching surges. In this paper the author, at first, intended to begin with the classified re-investigation of the above conditions and next to analyse switching surges due to small current interruption referring to a great number of oscillograms obtained in actual systems and thus he can conclude theoretically as well as experimentally a more accurate conceptions in this domain.

The following items should be fully discussed to clarify the switching phenomena from the point of view of the overvoltages.

- (1) The magnitudes, wave forms and natural frequencies of switching surges in actual systems.
- (2) The suppression of switching surges effected by the improvement of breaker characteristics and of system conditions.
- (3) The dielectric strength of insulations for switching surges.
- (4) The operation duty of lightening arresters for switching surges.
- (5) The testing method to assure the insulation coordination for switching surges.

Chapter 1. A Short Review on Switching Phenomena

There often happened explosion accidents of plain circuit breakers as the electric transmission lines had been grown up over rather expanded territories. Since then, the characteristics of circuit breakers have been improved in order to interrupt the large magnitude of current under faults, especially, the large short circuit current. The recent circuit breakers, however, must interrupt various sorts of currents to fit in with the advanced request of system operations, which may be classified in Fig. 1.1.¹⁾ The electric arc is always ignited between the contacts in case of the interruption of such current, and success or failure of the circuit interruption totally depends on that of arc quenching. Every maker in the world has designed and provided various types of circuit breakers, while such developements of the apparatus have been mainly supported only by "trial and error" method. Slepian successfully explained the interrupting process by a

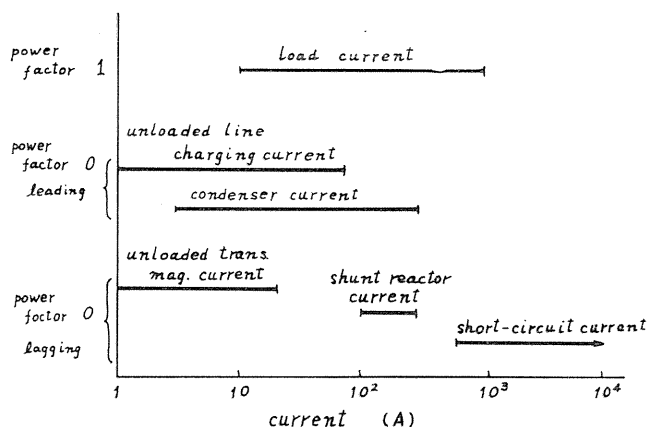


FIG. 1.1. Current to be interrupted in power systems.

rating model between the increasing rate of recovery voltage and that of dielectric strength after an arc extinction.²¹ There is no decisive theory on the physical mechanism of the interruption processes. The interruption of small current with low power factor now becomes the main subject of discussion from the view-point of switching surges. Such interrupting processes are frequently accompanied with switching surges and, thus, must be considered in order to satisfy the conditions of insulation coordination.

The fundamentals in case of the interruption of capacitive current were discussed, for example, in Hunt's paper³ and many theoretical analyses⁴⁻¹² and analogical researches¹³⁻¹⁷ have been carried out. At the same time there have been also published many oscillograms taken in the actual power systems.¹⁸⁻²⁰

There are many papers which treat the interruption phenomena of small inductive current.²¹⁻²⁵ Recently, Young's paper²⁶ and a report from Czechoslovakia²⁷ are published. And some papers dealt with the designing parallel resistances for the purpose of preventing from serious overvoltages.²⁸⁻³⁰ But any detailed discussion has not been referred to at the instant of current chopping.

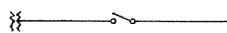
Unsatisfactory items in those published papers might be pointed out as follows.

- (1) Correlation between the arc quenching theory and the magnitude of switching surges.
- (2) Investigations of harmonic components in voltage and current.
- (3) Definition of reignition and restriking, especially, in uneffectively grounded systems.
- (4) Wave forms caused by reignition or restriking.
- (5) Time duration of arcs followed by reignition or restriking.
- (6) Types of reignition expected to occur.
- (7) Ranges of overvoltages expected to occur.

The author have resolved some of the problems above-mentioned by analysing the actual oscillograms which were experienced in test conditions shown in Table 1.1.

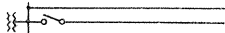
TABLE 1.1. Test Series

Substation	Interruption of capacitive current						Interruption of inductive current					Note
	System	Neutral	Circuit con- dition	Voltage (KV)	Current (A)	Number of test	Transformer	Voltage (KV)	Current (A)	Number of test		
										Perma- nent	Inrush	
Kakomachi	Under-ground cable	isolated	A B	30.6 ~ 32.4	4.3 ~ 5.3	24 23	—	—	—	—	—	ECB ×1 OCB ×3 in Feb. 1953
		resistance grounded 1000, 200, 37, 0 Ω	A B	31.0 ~ 32.4	4.4 ~ 5.2	18 16	—	—	—	—	—	
Yamaguchi- chō		isolated	A B	30.9 ~ 33.3	3.0 ~ 30.0	35 40	3 ϕ, 30/3 KV 6,000 KVA ×1	31.2 ~ 32.7	about 3	16	12	ABB ×2 in June 1954
Yokota		isolated	B	30.3 ~ 30.6	6.1 ~ 7.6	5	3 ϕ, 30/3 KV 6,000 KVA ×1	31.8 ~ 32.8	about 3	10	10	ABB in July 1954
Gokiso		isolated	A B	32.6 ~ 33.3	6.6 ~ 16.5	12 10	3 ϕ, 30/3 KV 6,000 KVA ×2	32.2 ~ 33.3	about 7	5	10	WCB in March 1955
Kasumori		isolated	A B	30.8 ~ 33.0	5.1 ~ 26.4	43 43	3 ϕ, 73.5/33 KV 30,000 KVA ×1	31.4 ~ 32.2	5.1 ~ 6.0	10	25	ABB ×2 in Dec. 1956
Tamagawa	Overhead line	resistance grounded 222.5 Ω	A B	70.0 ~ 73.0	9.6 ~ 37.2	80 97	3 ϕ, 154/77 KV 60,000 KVA ×1	71.0 ~ 72.0	about 3.5	29	42	CCB ×2 ABB ×2 OCB ×2 in March 1957
		isolated	B	69.0 ~ 70.5	11.5 ~ 18.0	19						



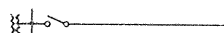
circuit condition type A

Kakomachi SS, Yamaguchi SS
Yokota SS, Gokiso SS
Kasumori SS



circuit condition type A

Tamagawa SS



circuit condition type B

Chapter 2. Interruption of Line Charging Current at Transformer Terminals with Isolated Neutral

§ 1. Experimental results

(1.1) Classification of actual reignition phenomena

The interrupting processes of small capacitive current, under the condition type B (cf. Table 1.1), may be classified into four types. (cf. Fig. 2.1)

Type I-a: This is a case in which the steady state charging current is interrupted most normally without any reignition or restriking in each line.

Type I-b: This is a case in which reignitions or restriking are happened to occur just after the temporary rupture of all lines according to Type I-a.

(Note) A reignition over two lines *a* and *b* is shown in Fig. 2.1 as an example, but any other sorts of reignitions may occur as are the cases with the following two conditions.

Type II-a: The three lines are rarely interrupted at the same time but each line is generally cleared up with proper time differences. This is a case in which reignitions or restriking may occur in the ruptured line while the others being still connected and the final clearing will be newly achieved. In an example of

Fig. 2.1, the arc is first quenched and is reignited again in phase *c*, while the other lines are still connected. Thus, all the conductions between contacts in three lines are revived and after some time the final rupturings are again achieved. It may be considered that a reignition will occur in phase *b* before arc in phases *a* and *c* are quenched. The Type II-a contains all such processes.

Type II-b: This is a case in which more reignitions or restriking are happened to occur just after the temporary rupturing of all lines according to Type II-a.

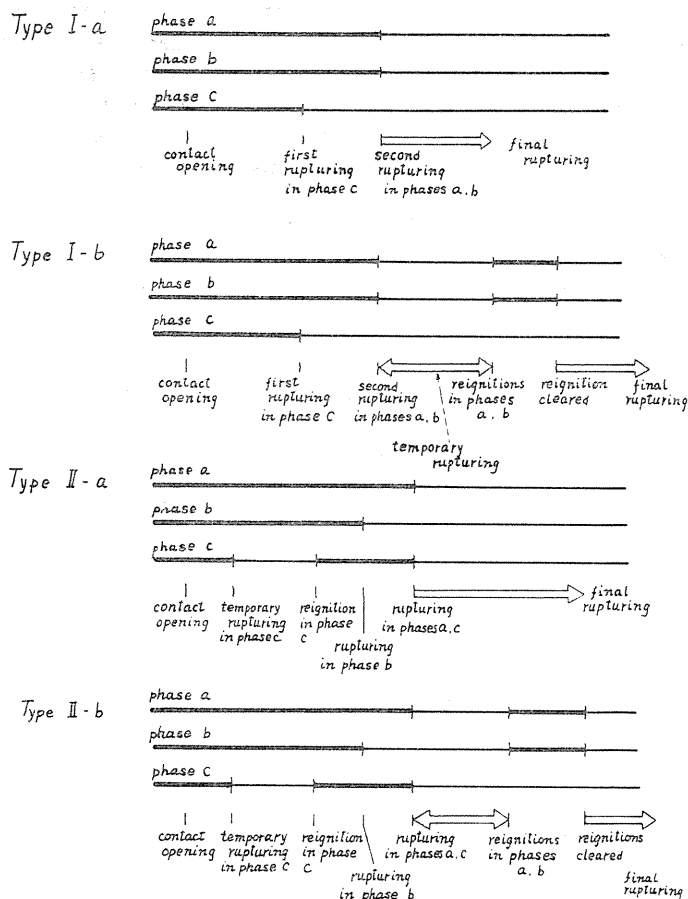


FIG. 2.1. Four types of interrupting processes of small capacitive current (circuit condition of type B).

The above-mentioned four types are all found in the interruption processes in resistance grounded systems, while Fig. 2.1 indicates four types in isolated neutral systems. It is characteristic in the latter systems, as shown in Fig. 2.1, that the arcs in two lines are always quenched at the same time. On the other hand, three arcs are generally interrupted one after another in the former systems. These are the only differences between the two cases. The relation between the

faculties of circuit breakers and these four types cannot be absolutely concluded. Circuit breakers with Type I-a, however, may be excellent ones. Circuit breakers with Type II-a may be considered as pretty good ones, unless successive reignitions or restriking occur alternately between lines temporarily quenched and the final interruption is remarkably postponed. Since the Type I-b or II-b means the slower and more irregular recovery of dielectric strength between the contacts, circuit breakers with such characteristics are not so desirable. Table 2.1 shows how the interruption processes of tested circuit breakers are assorted to those four types. The assortment is affected, on one hand, by the faculties of each breaker and, on the other hand, by the content of harmonics in voltage or current waves, etc. Total test numbers of each breaker under the circuit condition of type B are taken as 100% respectively, which makes it easy to compare a test result with the others. The column at the extreme right contains the actual test numbers. Forced-quenching circuit breakers (which are all air-blast circuit breakers here) are more apt to take the process of Type I-a than self-quenching circuit breakers, but circuit breakers No. 5 in Kasumori SS and No. 6 in Tamagawa SS show exceptional characteristics. In this paper the word "reignition" is used as a simple expression, which contains both so-called reignition and restriking. The following discussion is mainly derived from the results obtained in Type I.

TABLE 2.1. Interrupting Processes of Circuit Breakers Tested

Sub station	circuit breaker	interrupting process				total	
		Type I-a	Type I-b	Type II-a	Type II-b		
Kakomachi	Self-quenching type	A	0%	100%	0%	0%	5 cases
		B	0	20	0	80	"
		C	80	0	20	0	"
		D	0	0	60	40	"
		No.4	0	25	12.5	62.5	8
Yamaguchi-Yokota	Self-quenching type	No.1	90	0	10	0	20
		No.2	80	0	20	0	"
		No.3	40	60	0	0	5
		No.4	70	25	5	0	20
Kasumori	Forced-quenching type	No.5	0	57	0	43	21
		No.2	50	50	0	0	6
Tamagawa	Forced-quenching type	No.6	0	20	0	80	5

(1.2) *Phase angles when an arc in each line is easily quenched*

The first rupturing of the sinusoidal capacitive current is normally achieved at the crest of phase voltage, that is, at 90° or 270° , where the time lapse is shown by phase angles from the zero passage of the voltage concerned. The circuit conditions of the interruption at 270° are essentially the same as those at 90° except the polarity. This rupturing time is experimentally related with the types of circuit breakers and the wave forms of the current ruptured. The Fig. 2.2(a) shows the distribution of the first rupturing time in Kasumori SS. The charging current in this test contains less higher harmonics and has the periodic normal zero passages indicated by wedge-shaped signs in Fig. 2.2(b). In the abbreviations as B-20 or B-25, the first "B" signifies the circuit condition of type B, and the following number expresses the approximate amount of the current interrupted in amperes. The first rupturing is never accomplished in the neighbourhood of 0° or 180° but, in most cases, of 70° to 80° , which is a little earlier than 90° . This seems to show an effect of the premature interruption peculiar to the air-blast circuit breakers. The current in Tamagawa SS contains more harmonics and its form is far from sinusoidal as shown in Fig. 2.3(c). The first rupturing time is recorded in great dispersity over the whole angles in both self- and forced-quenching breakers. Three wave forms in Fig. 2.3(c) contain mainly the 5th harmonics almost in the same manner. Fig. 2.4 is the detailed wave form of the current of B-30. The times of zero passage derived from this analysis are indicated by wedge-shaped signs at the bottom of Figs. 2.3(a) and (b), which reveal the distribution characteristics of first rupturing time for various circuit breakers in Tamagawa SS. It is obviously found that experienced numbers of times ruptured correspond to those zero passages. As to the influence

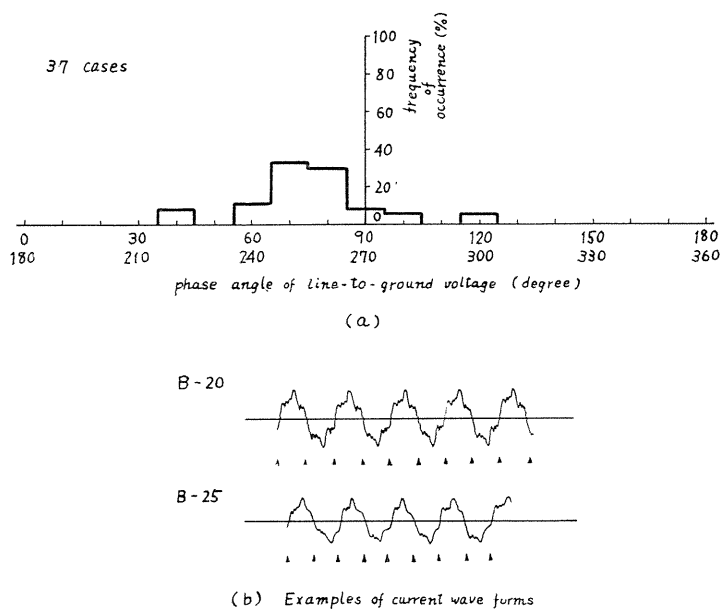
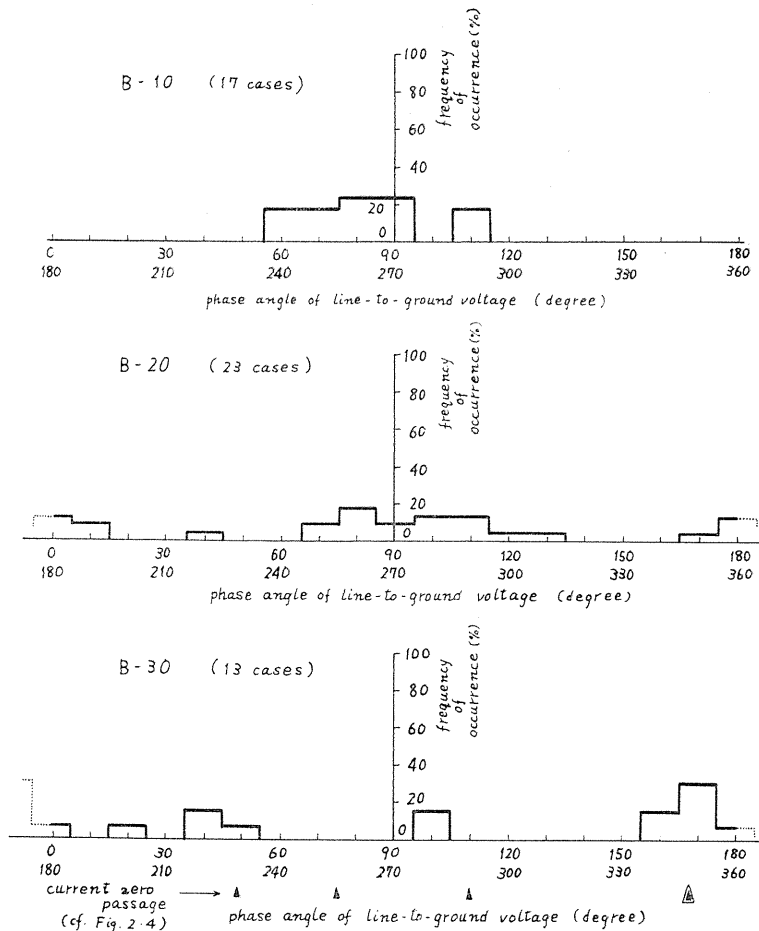


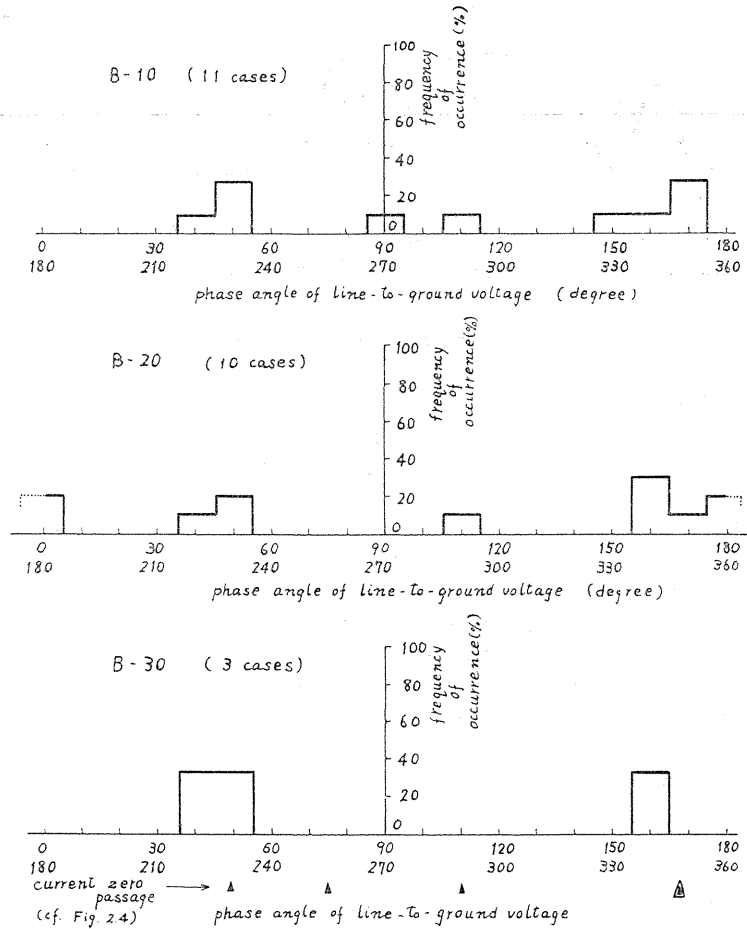
FIG. 2.2. Phase angles at the first rupturing. Forced quenching type circuit breaker (ABB) in Kasumori SS. Isolated neutral.

of the types of circuit breakers, the distribution is almost the same for each current magnitude in case of forced-quenching circuit breakers, whereas, in case of self-quenching circuit breakers, it is affected by the current magnitude, that is, the first rupturing time falls between 60° and 110° (or 240° and 290°) in relatively lower values of currents and then comes to separate into the neighbourhoods of four zero passages indicated, especially at 168° (or 348°). Although the current does not come to zero at 168° (or 348°) in B-10, it nearly keeps zero value for a considerably long period at the time shown by \blacktriangle in B-30, in which the other zero passages marked by \blacktriangle are instantaneously passed through by crossing instead of osculating in the curves demonstrated. Therefore, the rupturing at the former point must be achieved more easily.

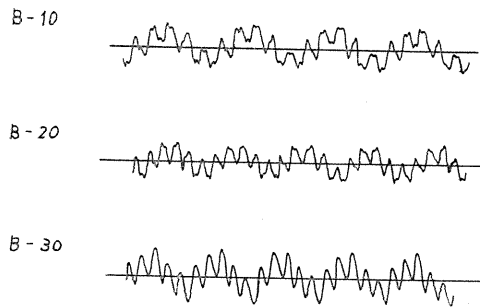
It may be derived from the above-mentioned facts that the chance for current quenching depends strictly upon the current zero passage in both cases of forced- and self-quenching circuit breakers and consequently, the period, during which



(a) Self-quenching type circuit breaker in Tamagawa SS resistance grounded system



(b) Forced quenching type circuit breaker in Tamagawa SS resistance grounded system



(c) Examples of current wave forms

FIG. 2.3. Phase angles at the first rupturing.

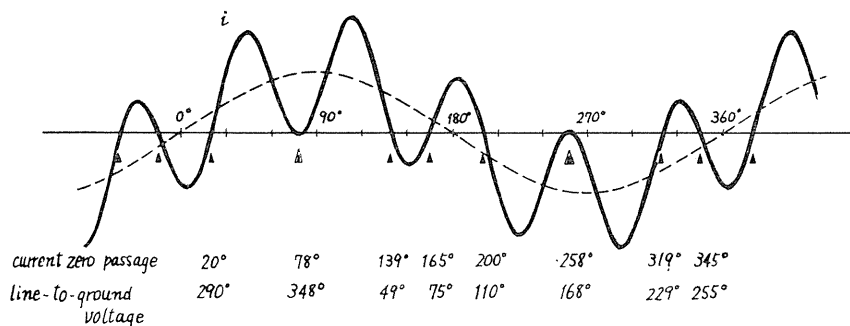
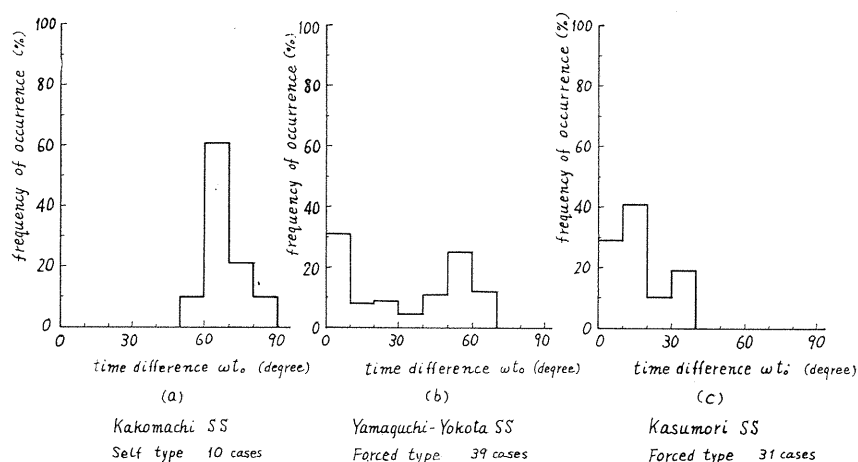


FIG. 2.4. Detailed current wave form of B-30 in Tamagawa SS.

the current keeps minute values, may be also a chance for forced quenching (concerning exclusively the air-blast circuit breakers).

After the current in one line is ruptured at first, the currents in the other two are never interrupted one after another but always cut off at the same time in an isolated neutral three-phase system. In the following discussion, the expression of the "second rupturing" is used to mean the interruption of such remaining currents in two lines. This second rupturing is achieved within some lapse of time after the first one is over, except the case of the simultaneous interruption of three line currents. In this respect each circuit breaker differs greatly from one another in its performance. Fig. 2.5 shows the examples of distribution of such time differences. Self-quenching circuit breakers, tested in Kakomachi SS, as shown in Fig. 2.5(a), attain to the second rupturing after the first one within 60° to 80°, the average values of which being 68°, that is shorter than 90° by 22°. Those time differences in Yamaguchi-Yokota and Kasumori SS's are shown in Fig. 2.5(b) and (c). Both diagrams equally show a large number of cases of interruption between 0° and 20°, while the distribution form of each case is quite peculiar. The distribution in Yamaguchi-Yokota SS has double peaks,

FIG. 2.5. Time difference ωt_0 between the first rupturing and the second rupturing.

one is between 0° and 20° , the other between 50° and 60° . The distribution in Kasumori SS is more biased towards the left hand side. The simultaneous interruption of three line currents or the interruption with shorter time difference is often realized in case of the small current. It is noteworthy that this investigation is wholly inconsistent with the so-called typical conception that the second rupturing would be achieved at 90° after the first.

The trapped voltage on lines after the final interruption depends on the time when the current in each line is quenched. An example is shown in Fig. 2.6, the abscissa of which indicates the trapped voltage normalized by the crest of the phase voltage, and along the ordinate of which are arranged the absolute values of the trapped voltage shown by the sign \bullet in their sequential magnitude. The polarity of the trapped voltage is denoted by that in the line ruptured at first. For example, if that is positive, the polarity in each line is recorded as itself, and if negative, recorded inversely. The former corresponds to the case where the first rupturing is achieved in the neighbourhood of 90° of the phase voltage, the latter to the case where it is done in the neighbourhood of 270° . In the case of the simultaneous interruption of three line currents, the polarity is so chosen as to adopt that of the nearest to 90° or 270° of the three. Although every trapped voltage in the first rupturing nearly holds the crest value of the phase voltage, those in the second represent the interesting forms on the diagram. The points, which are arranged only according to the sequence of the absolute value of the sign \bullet , result in nearly symmetrical arrangement of the points designated by \odot with the ordinate of $-0.5E$ as the symmetrical axis. The signs of \odot lie nearly along the dotted line which links exactly the symmetrical position to the signs \bullet . In case of the interruption with greater time difference between

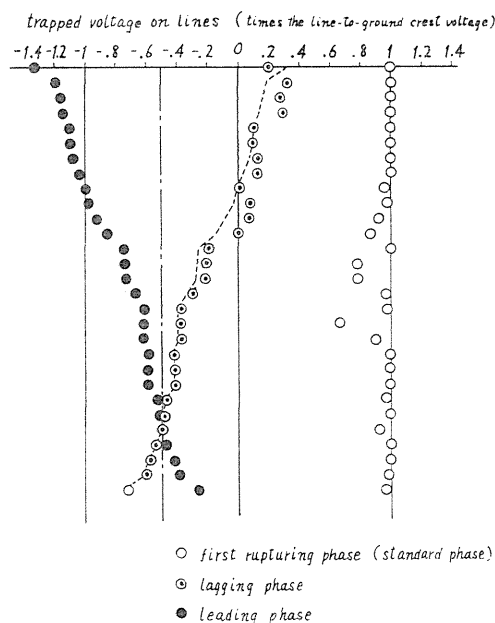


FIG. 2.6. Trapped voltage on lines (Yamaguchi-Yokota SS).

the first rupturing and the second, the trapped voltage on the lagging phase to the first one is calculated by $-0.5 E + V$ ($V \geq 0$), whereas one on the leading phase is denoted by $-0.5 E - V$ ($V \geq 0$). But these two signs intercross in the lower part of the figure. Such situation is caused when the three line currents are all interrupted simultaneously near at 90° of a phase voltage.

(1.3) *Observed sequences of reignitions*

Table 2.2 shows in which phase the initial reignition occurs between the contacts after the steady capacitive current are temporarily interrupted. Although these investigations require precise tracings of oscillograms of the voltage across the contacts, the actual trigger voltage cannot be distinguished when the reignitions in two or three lines start nearly at the same time. The construction of this table is as follows; "Circuit breaker" is classified into two types, *i.e.* "Self-quenching type" and "Forced-quenching type", "Substation" indicates the substations where the tests were carried out, "Interrupting process" contains the Types I-b and II-b, considering the trapped voltage and the shifted voltage of the neutral potential-to-ground in the source side of the breaker are quite different between Type I and II, and "Line of initial reignition" is classified into the first, the lagging and the leading phase. In case of the simultaneous interruption, however, the standard phase is assumed as the phase the current in which is interrupted at the nearest of normal zero passage. This table indicates that the dielectric strength between the contacts in the second ruptured lines seems to be weaker, *i.e.* the dielectric strength between the contacts with longer burning period of arc is apt to be broken fast. During this investigation it is

TABLE 2.2. Line of Initial Reignition After the Second Rupturing

Circuit breaker	Substation	Interrupting process	Line of initial reignition				Total (cases)
			first rupturing (cases)	lagging phase (cases)	leading phase (cases)	unknown (cases)	
Self-quenching type	Kako-machi	Type I-b	2	1	2	1	6
		Type II-b	2	1	2	1	6
		sum (%)	4(33)	2(17)	4(33)	2(17)	12(100)
	Tamagawa	Type I-b	1	0	0	1	2
		Type II-b	1	3	1	0	5
		sum (%)	2(29)	3(43)	1(14)	1(14)	7(100)
Forced-quenching type	Yamaguchi-Yokota	Type I-b	0	3	0	0	3
		Type II-b	0	0	0	0	0
		sum (%)	0(0)	3(100)	0(0)	0(0)	3(100)
	Kasumori	Type I-b	1	10	2	4	17
		Type II-b	0	4	4	1	9
		sum (%)	1(4)	14(54)	6(23)	5(19)	26(100)
	Tamagawa	Type I-b	1	2	1	0	4
		Type II-b	0	1	3	0	4
		sum (%)	1(12.5)	3(37.5)	5(50)	0(0)	8(100)

not recognized that the insulation between the contacts in a particular line would be always broken at first, so that, the tendency above-deduced cannot be the result from the irregular separation of the moving contacts. This tendency is commonly recognized in both Types I-b and II-b. And, moreover, the dielectric insulation in the lagging phase is weaker than in the leading except in cases of self-quenching circuit breakers in Kakomachi SS and the forced-quenching ones in Tamagawa SS. The number of times, that the initial reignition occurs between the contacts in the first rupturing, is larger in the self-quenching circuit breakers than in the forced-quenching and it amounts up to 33% in the former while 12.5% at most in the latter.

No reignitions occur after the final rupturing in the Type I-a and II-a but at least one reignition occurs after the temporary rupturing of three lines in the Type I-b and II-b. A reignition between the contacts in a line may induce reignitions in one of the other lines or both of them. The former is here called the "two-phase reignition" and the latter the "three-phase reignition". The case is also possible in which an initial reignition does not induce any reignition but is quenched. Such case is called the "single-phase reignition". Table 2.3 shows the result of the investigation of these induced reignitions. The expressions of three columns in the left side are the same as those of Table 2.2. The "First reignition" shows the number of frequencies of three styles of reignition which are first induced after the temporary rupture of current in three lines. The following three sections to the right, each consisting of three columns, refer to the

TABLE 2.3. Reignition Types

Circuit breaker	Substation	Inter-rupting process	First re-ignition (cases)			Reignition succeed (cases)									Summerized result (cases)			Total (cases)
			over 3 lines	over 2 lines	over 1 lines	after 3-phase re-ignition			after 2-phase re-ignition			after a single phase re-ignition			over 3 lines	over 2 lines	over 1 lines	
						over 3 lines	over 2 lines	over 1 lines	over 3 lines	over 2 lines	over 1 lines	over 3 lines	over 2 lines	over 1 lines				
Self-quenching type	Kako-machi	Type I-b	4	0	2	1	3	2	0	1	1	1	1	0	6	5	5	16
		Type II-b	2	4	0	0	4	0	2	4	0	0	0	0	4	12	0	16
		sum(%)	6	4	2	1	7	2	2	5	1	1	1	0	10 (31.5)	17 (53)	5 (15.5)	32 (100)
	Tama-gawa	Type I-b	1	1	0	0	1	0	1	0	0	0	0	0	2	2	0	4
		Type II-b	1	4	0	0	1	0	0	1	0	0	0	0	1	6	0	7
		sum(%)	2	5	0	0	2	0	1	1	0	0	0	0	3 (27)	8 (73)	0 (0)	11 (100)
Forced-quenching type	Yama-guchi-Yokota	Type I-b	1	2	0	0	0	0	0	1	0	0	0	0	1	3	0	4
		Type II-b	0	0	0	0	0	0	0	0	0	0	0	0	0	0	0	0
		sum(%)	1	2	0	0	0	0	0	1	0	0	0	0	1 (25)	3 (75)	0 (0)	4 (100)
	Kasu-mori	Type I-b	10	7	0	2	4	1	6	3	0	0	0	0	18	14	1	33
		Type II-b	5	4	0	3	4	0	4	1	0	0	0	0	12	9	0	21
		sum(%)	15	11	0	5	8	1	10	4	0	0	0	0	30 (55.5)	23 (42.5)	1 (2)	54 (100)
Tama-gawa	Type I-b	0	2	2	0	0	0	0	0	1	0	0	0	0	2	3	5	
	Type II-b	0	3	1	0	0	0	0	0	0	0	0	0	0	3	5	8	
	sum(%)	0	5	3	0	0	0	0	0	1	0	0	0	0 (0)	5 (38.5)	8 (61.5)	13 (100)	

Note: * A singular case with successive single phase reignition.

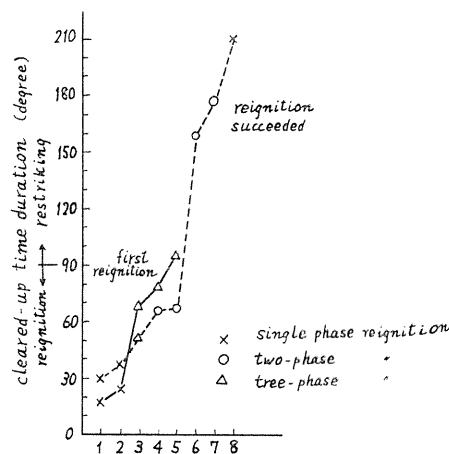
correlation between the successive reignitions after the first one. The total number of frequencies are listed in the section of the extreme right.

In this table one can recognize the two-phase and three-phase reignitions are often found in an isolated neutral system. This tendency is also the truth with respect not only to the first re-ignition but to the successive ones. The two-phase re-ignition follows in most cases after the first re-ignition. But, in case of Kasumori SS, a two-phase re-ignition is apt to be caused after the quenching of a three-phase re-ignition, and a three-phase one after a two-phase. After the initial re-ignition is caused in a line, the potential-to-ground of source side is changed remarkably. This change gives rise to a remarkable influence on the recovery voltage between the contacts in the other two lines. If such a transient recovery voltage overtakes the dielectric strength between them, a new arc reignites. Table 2.4 shows which of the two phases is liable to be combined together with the other by such a transient voltage. The manner of tabulation is the same as that of Table 2.2. Such induced re-ignition is generally caused in one of the second ruptured lines.

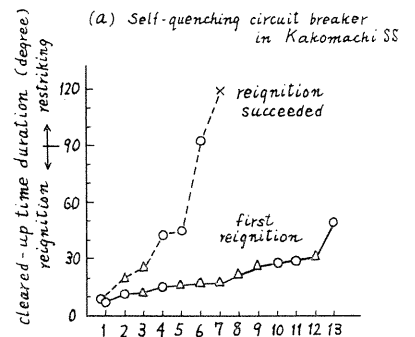
Fig. 2.7(a) and (b) indicate the examples of the time interval between a rupturing and the following re-ignition with respect to Type I-b. The "cleared-up time duration" is expressed by the cleared-up time of the phase in which an

TABLE 2.4. Combination of Two-phase Re-ignition

Circuit breaker	Substation	Interrupting process	Combination (cases)			Total (cases)
			first rupturing + lagging phase	first rupturing + leading phase	lagging phase + leading phase	
Self-quenching type	Kakomachi	Type I-b	0	0	0	0
		Type II-b	0	2	2	4
		sum(%)	0	2	2	4
			(0)	(50)	(50)	(100)
Self-quenching type	Tama-gawa	Type I-b	0	0	1	1
		Type II-b	0	0	4	4
		sum(%)	0	0	5	5
			(0)	(0)	(100)	(100)
Forced-quenching type	Yama-guchi-Yokata	Type I-b	1	0	1	2
		Type II-b	0	0	0	0
		sum(%)	1	0	1	2
			(50)	(0)	(50)	(100)
	Kasumori	Type I-b	2	0	5	7
		Type II-b	0	0	4	4
		sum(%)	2	0	9	11
			(18)	(0)	(82)	(100)
Forced-quenching type	Tama-gawa	Type I-b	0	0	2	2
		Type II-b	0	0	3	3
		sum(%)	0	0	5	5
			(0)	(0)	(100)	(100)



(a) Self-quenching circuit breaker in Kakomachi SS



(b) Forced quenching circuit breaker in Kasumori SS

(Note) abscissa : one point for one case

FIG. 2.7. Cleared-up time before a re-ignition.

initial reignition occurs. The longer are the time intervals, the farther to the right are situated the corresponding points. According to the established practice, the reignition with the time interval longer than 90° is called "restriking" and shorter than 90° "reignition", which are formally distinguished in the ordinate of the figures. Three styles of reignition are denoted by three different marks as shown. Most of the first reignitions are caused within 30° just after the previous rupturing and few restrikses beyond 90° in case of this forced-quenching circuit breaker and the tendency is also valid in circuit breakers of the same sort, while the first reignitions are caused over the wide range below 90° in case of self-quenching circuit breakers. The corresponding time interval is also investigated with respect to the successive reignitions. Some restrikses appear in Fig. 2.7(a) and several reignitions are found at the time longer than 30° in Fig. 2.7 (b). With longer time intervals, three-phase reignitions cease to occur, and, on the other hand, the unfavourable single-phase reignitions come to exist.

(1.4) Arc duration time and circuit characteristics

The burnning period of reignited arc seems to have some relation with the preceding cleared-up time. Since the preliminary investigation for each circuit breaker indicates, in this regard, a common tendency, Table 2.5 is generally accepted as the final result, in which the number of total reignitions in each test is estimated as 100% respectively. As a transient wave form of voltage during a reignition is generally oscillating, the burnning period may be denoted by the multiples of its loop. This table consists of three domains, designated by *A*, *B* and *C*. Most of reignitions belong to the domain *A*. The reignitions with the burnning period of 0.5 cycle of the transient oscillation are occasionally found, almost all of which are effected within 60° after the previous quenching. The table shows that a reignition after a longer cleared-up time has a tendency to sustain an arc for a longer duration of time. There is no reignition belonging to the domain *B* so far as this investigation is concerned. The reignition within

TABLE 2.5. Time Duration of Reignition (isolated neutral system)

Cleared-up time (degree)	Time duration (cycles of natural frequency)					
	sparkling *	0.5	1	1.5	2	2.5 and over
0- 30°	6.4%	25.2%	2.1%	1.1%	0.6%	5.9%
31- 60°	3.6	21.1	2.6	3.3	1.7	0.3
61- 90°		1.1	1.0	1.1	3.2	4.1
91- 120°	0.1	4.4		0.1	1.1	0.3
121- 150°		2.4		0.6	0.8	2.2
151- 180°		2.2			0.8	0.3
181- 210°	(domain C)		(domain B)			
211- 240°	0.3					
241° and over						

Note: 264 reignitions in total * cf. Fig. 2.10(b)

the domain C is one of the sources of overvoltages and 10% of the cases investigated belong to this domain. A reignition after the cleared-up time of between 211° and 240° causes a remarkable shift of the neutral-to-ground potential. An overvoltage due to the cumulative trapped voltage on the capacitive element may be realized when reignitions belonging to this domain are caused successively more than two times, but, according to this table, such circumstances are rarely brought about. Within the result of this investigation only two cases were encountered with.

The frequency of the transient voltage and current after reignitions can be well estimated with considerable accuracies but their damping factor with great difficulties. Thus, the correlation between the damping time constant τ and the frequency f is experimentally investigated for each oscillation with a typical form of a single frequency. The quality factor Q for resonance in power systems can be also estimated, regarding the network as a single L - C - R series circuit, equivalently. The empirical formulae obtained are

$$\left. \begin{aligned} \tau &= \frac{1120}{f^{0.9}} \quad (\text{msec}), \\ Q &= 3.52 f^{0.1} \end{aligned} \right\} \quad (1)$$

respectively. The corresponding charts are shown in Figs. 2.8 and 2.9.

Two examples of reignitions are shown in Figs. 2.10(a) and (b). (a) is a typical reignition over two lines: phases a and c . The detailed process is as follows. The dielectric insulation between the contacts in phase c is broken down at first and it results in the induced jumps of voltages-to-ground in phases a and b . During the course of such jump the dielectric insulation between the contacts in phase a can not withstand such transient recovery voltage and then

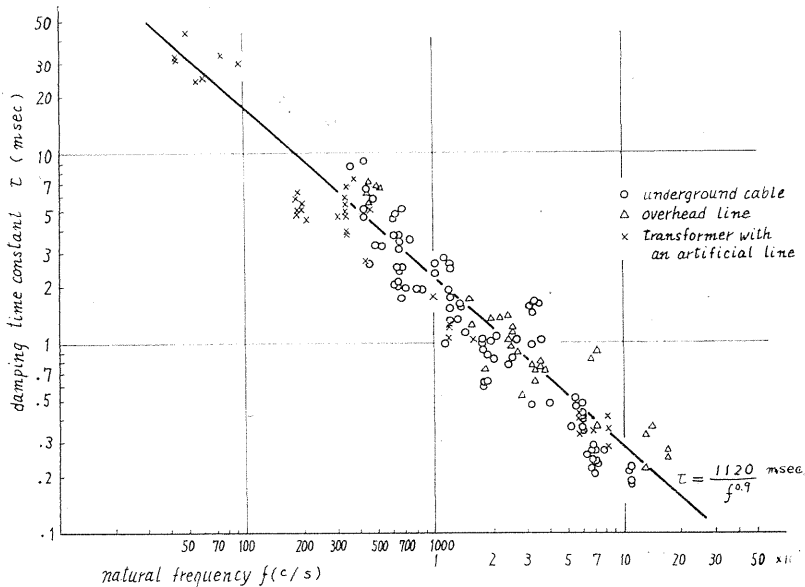
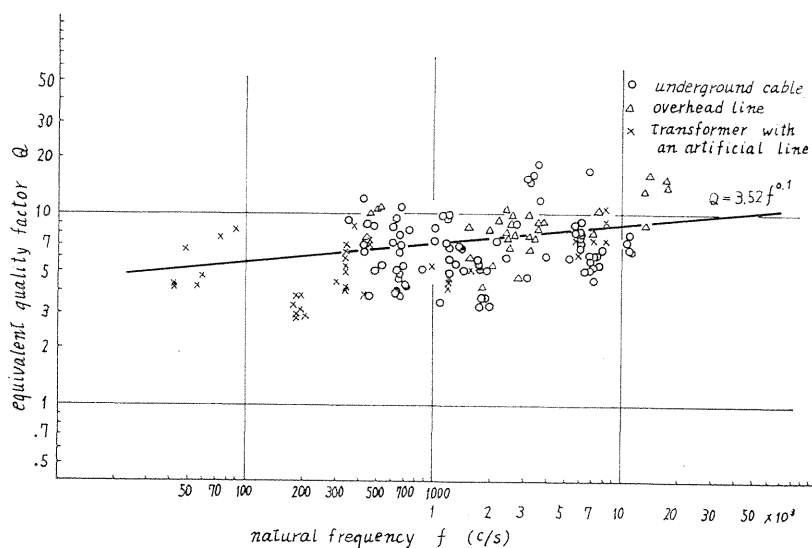


FIG. 2.8. τ - f characteristic.

FIG. 2.9. Q - f characteristic.

is broken down. Thus a typical reignition over two lines are caused. (b) is a reignition in a single line, which is quenched within a very short time duration, not inducing any other reignition, which is called as the sparking reignition in the following discussion. The trapped charge passes through the arc path into the bus conductor so as to cause a sustained voltage shift of the source potential. As shown in Fig. 2.10(b), the amount of this shift is just equal to the instantaneous recovery voltage before the reignition. As the result of the voltage shift of $1.5 E$, the crest voltage in each line reaches and sustains $2.5 E$ with the system frequency.

§ 2. Theoretical investigations on reignition phenomena

The first rupturing is achieved in the neighbourhood of 90° of the phase voltage and even in case of a premature interruption that point is advanced only by 10° to 20° , while the periods between the first rupturing and the next distribute irregularly over 0° to 90° . Although the self-quenching circuit breakers, tested at Kakomachi SS, were made in the beginning of the 1950's, those periods fall between 60° and 70° , which are shorter than 90° by more than 20° . The reason is easily explained by the fact that the remaining single phase circuit is interrupted by two points in series. The forced-quenching circuit breakers have the shorter arcing periods in general and often interrupt all three currents at the same time. The circumstances during an interruption of capacitive current under the circuit condition type B may be expressed schematically as Fig. 2.11.

From various investigations of the line charging current interruption, it may be concluded that a recovery voltage in each line contains less high frequency components but mainly consists of fundamental component. And the very small capacitance C_s remaining on the source side is of a great significance for the final interruption. From the theoretical point of view, C_s may be an imaginary

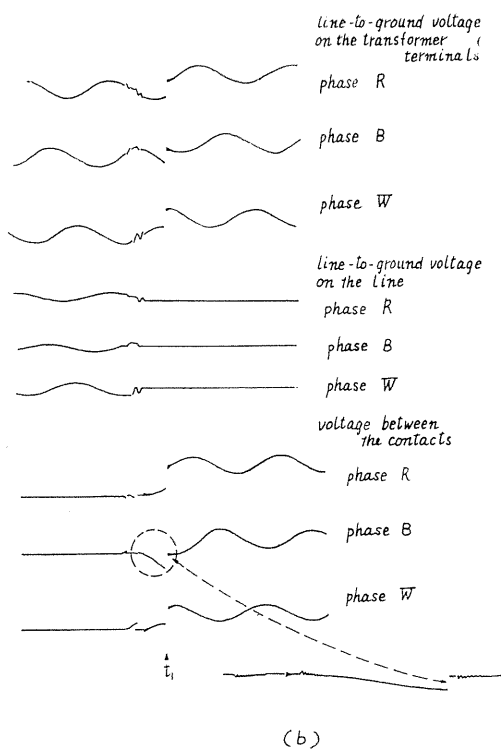
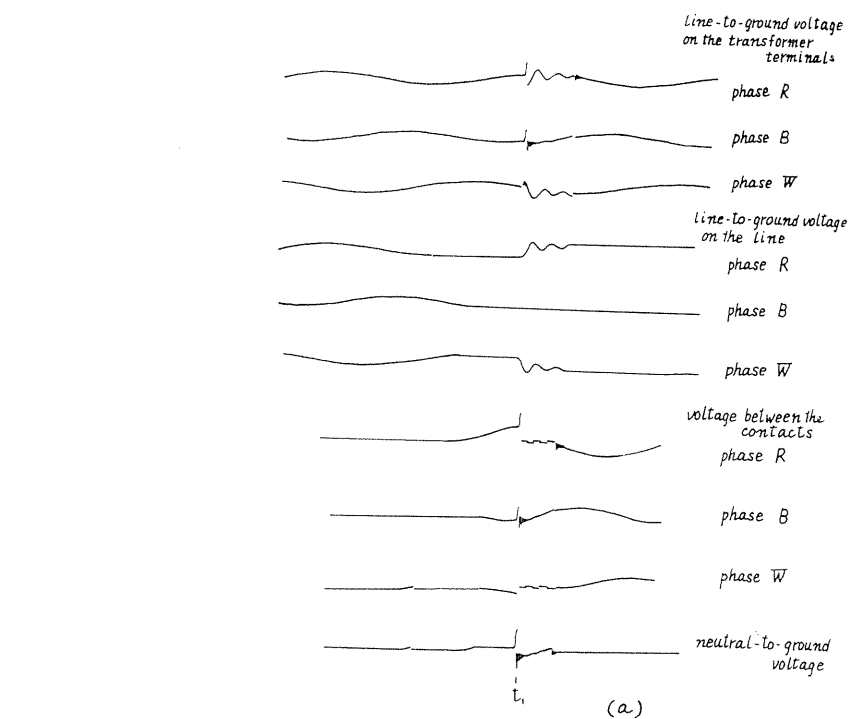
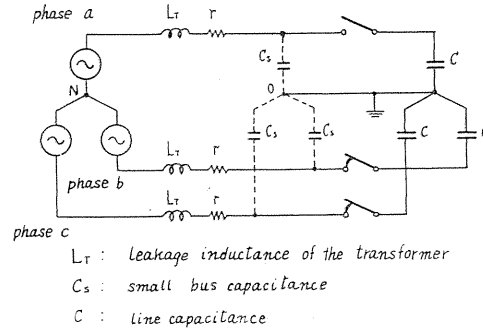


FIG. 2.10. Two examples of reignition phenomena in 30 kV cable system with isolated neutral.

(a) Voltage transient caused by the initial reignition in phase W, and induced reignition over two lines of phases R and W.

(b) Neutral-to-ground potential shift caused by a sparking reignition in phase B.

FIG. 2.11. Schematic circuit diagram during the interruption of capacitive circuit of types B.



capacitance as the position of a circuit breaker approaches to the end of a line as a limiting case, but in practice a small capacitance always remains on the bus conductor. This small capacitance plays an important role in the oscillatory jumps of voltages after a reignition, in the sustaining potential shift after a sparking reignition, and in the neutral potential-to-ground after a final interruption. The trapped voltage on the line is thus affected by these factors. In the following calculation, the quantities referred to each of the three lines are represented by suffixes of a , b and c according to the positive phase sequence. The trapped voltage on each line is given as follows.

$$\left. \begin{aligned} E_{0a} &= E, \\ E_{0b} &= -0.5 E + 0.866 E \sin \omega t_0, \\ E_{0c} &= -0.5 E - 0.866 E \sin \omega t_0, \end{aligned} \right\} \quad (2)$$

where the phase a is taken as the first phase; the electrical angle θ'_a of the voltage in phase a is just 90° at the first rupturing, and the rupture of current in phases b and c is achieved after the time lapse of t (sec); $C_s \ll C$, E is the crest value of the phase voltage, $\omega = 2\pi f_0$, f_0 is the system frequency.

Eqs. (2) indicate that the trapped voltages in phases b and c take the symmetrical magnitudes with $-0.5 E$ as the axis. And these equations are also available if θ'_a is chosen in the neighbourhood of 90° instead of just 90° . With the simultaneous interruption of all the currents, the trapped voltage in each line is nearly equal to the instantaneous value of respective phase voltage. Even in

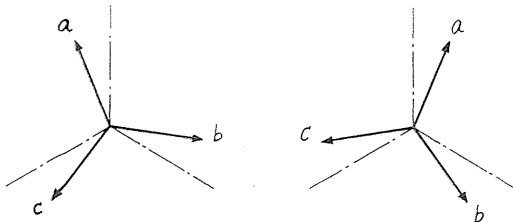


FIG. 2.12. Vector diagram of line-to-ground voltage at the simultaneous interruption in three lines.

such case if an angle of a line voltage is near 90° , the values of the trapped voltages in the other two keep the symmetrical relation on both sides of $-0.5 E$, as shown in Fig. 2.12, which also indicates that the trapped voltages in the leading phase and in the lagging one interchange their amounts according to $\theta'_a < 90^\circ$ or $\theta'_a > 90^\circ$.

After the final or the temporary interruption the neutral potential of the source side has some shift voltage V_0 with DC component due to the trapped charge in C_s . In case of $\theta'_a = 90^\circ$ and with the time interval t_0 , V_0 is given as

$$V_0 = -0.5 E(1 - \cos \omega t_0), \quad (3)$$

and in case of a simultaneous interruption in three lines,

$$V_0 = 0. \quad (4)$$

According to Eq. (3), each line-to-ground voltage in the source side is given as

$$E_\kappa = E \sin(\omega t + \theta'_\kappa) + V_0, \quad (5)$$

where $\kappa = a, b$ and c , $\theta'_a = (\pi/2) + \omega t_0$, $\theta'_b = -(\pi/6) + \omega t_0$, $\theta'_c = (7\pi/6) + \omega t_0$, and θ'_κ is equal to the instantaneous angle of each phase voltage just when the arc extinction is achieved. The recovery voltage is derived by the difference between the line-to-ground voltage in the source side and the trapped voltage on the line. According to the actual investigations mentioned in previous section, the interrupting process may be classified into five typical patterns as the combination of θ'_a and ωt_0 like $(\theta'_a, \omega t_0)$. They are

$$(90^\circ, 90^\circ), (90^\circ, 60^\circ), (90^\circ, 30^\circ), (90^\circ, 0^\circ) \text{ and } (60^\circ, 0^\circ).$$

A series of the recovery voltages for each line are traced in Fig. 2.13 taking every arc extinction point as the common origin.

The initial recovery voltage in phase a always build up along the line \widehat{OA} before the second rupturing in the other two phases is effected, and the first possible crest value will decrease as the time t_0 become shorter. The recovery voltage of phase a arrives at the point A when the currents in phases b and c are interrupted at $\omega t_0 = 90^\circ$ assuming $\theta'_a = 90^\circ$. The corresponding point A at every instant earlier than $\omega t_0 = 90^\circ$, lies on the line \widehat{OA} according to its abscissa. With larger values of ωt_0 , the recovery voltage across the contacts in phase a reaches rather high voltage by the time of the second rupturing. In case of $(60^\circ, 0^\circ)$, the recovery voltage in phase a shows once a low maximum at the beginning but the severity impressed across the contacts is not so great in spite of a little higher rate of rise. Next, the superposition of \widehat{OA} on the traces in phases b and c , drawn by dotted lines in Fig. 2.13, shows that the recovery voltages in phases b and c are evidently higher than \widehat{OA} . Restricting the discussion to the interrupting process of Type I, the recovery dielectric strength must be higher than \widehat{OA} in phase a but the recovery rates in phases b and c are seemed to be comparative with the rate of \widehat{OA} , because many initial reignitions are actually caused in phase b or c as shown in Table 2.2.

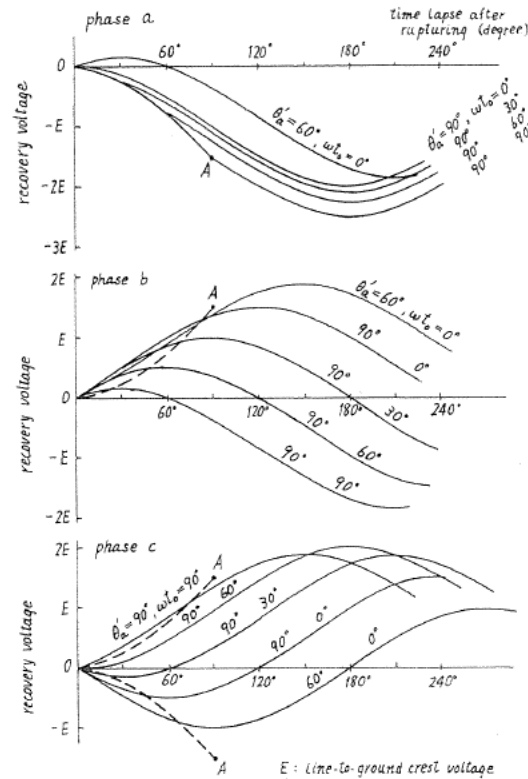


FIG. 2.13. Recovery voltages.

§ 3. Theoretical investigations on overvoltages accompanied with reignitions

(3.1) Initial reignition

An initial reignition suddenly renders a bus voltage equal to the trapped voltage on the line. In Fig. 2.11, C is schematically connected with C_s in parallel by this reignition and the terminal voltage of the parallel connected capacities becomes equal to the trapped voltage across C , independent of the instantaneous voltage across C_s as the capacity of C is much larger than C_s . This reignition in phase a results in the initiation of greatly magnified voltage transient both on the terminals in phases b and c . Since L_r and r may be neglected compared with C , Fig. 2.11 may be transformed to Fig. 2.14. In this figure, the transient phenomena may be analysed for each of the branches $a-b$ and $a-c$, respectively. The original equations in section (3.5) results in

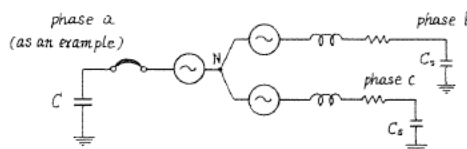


FIG. 2.14. Schematic circuit diagram during the initial reignition.

$$\left. \begin{aligned} E_{c1} &= \sqrt{3} E \sin(\omega t + \theta' \mp 5\pi/6) + (E \sin \theta' + V_0 + E_{02})e^{-t/\tau} \cos \nu t - E_{02} \\ E_{c2} &= E_{02} \end{aligned} \right\} \quad (6)$$

where E_{c1} is the voltage across C_s in phase b or c , E_{c2} is the voltage across C in phase a (cf. Fig. 2.14), referring their direction to the section (3.5), and the instant of a reignition is taken as the origin of the time t , and the angle of each phase voltage at $t=0$ is indicated by θ' . The initial voltage across C_s is given by Eq. (5) and the initial voltage E_{02} across C in the reignited phase is given by Eqs. (2) as the trapped voltage after the previous rupturing. The upper sign in the equation corresponds respectively to the lagging phase and the lower sign to the leading phase with regard to the reignited phase. Eqs. (6) indicate that the line-to-ground voltage initiates a voltage transients with a cosine-like wave-front from the instantaneous value with the frequency of $\nu/2\pi$ (c/s). The maximum overvoltage is realized at its crest, which can be derived by putting $t=\pi/\nu$. Since the frequency accompanied with the initial reignition is generally high, the variation can be neglected for the fundamental phase voltage during this period. The first crest $E_{c1 \max}$ is given as

$$E_{c1 \max} = \sqrt{3} E \sin(\theta' \mp 5\pi/6) - k(E \sin \theta' + V_0 + E_{02}) - E_{02},$$

that is

$$E_{c1 \max} = -E \sqrt{\left(\frac{3}{2} + k\right)^2 + \left(\frac{\sqrt{3}}{2}\right)^2} \sin(\theta' \pm \chi) - kV_0 - (1+k)E_{02}, \quad (7)$$

where $\tan \chi = \frac{\sqrt{3}}{2} / \left(\frac{3}{2} + k\right)$. The first term in Eq. (7) is independent of the trapped voltage and equivalent to the first crest value induced in the other phases

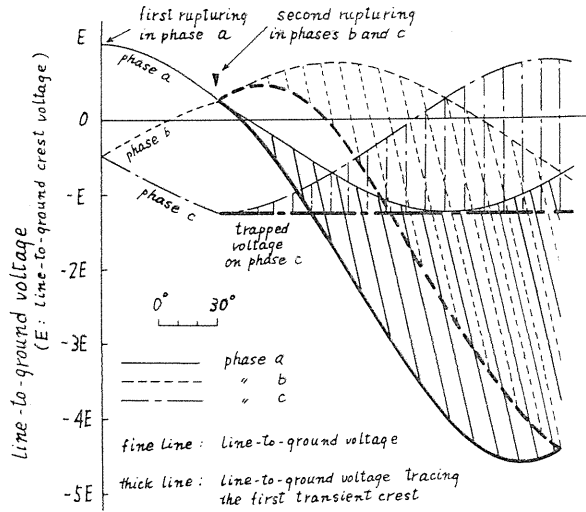


FIG. 2.15. Line-to-ground overvoltage caused by the initial reignition in phase c , when the steady state capacitive current is interrupted by the pattern of $\theta'_a=90^\circ$, $\omega t_0=60^\circ$.

due to a premature closing. Eq. (7) plotted with θ' as a variable is nothing but the curve connecting every crest and shows a limit of the overvoltage of this kind. Many experiments show the frequency accompanied with this reignition is usually within the range between 2 and 5 kc/s. Fig. 2.15 is an example of a limit of this first crest with 4 kc/s as a model frequency for the case of $(\theta'_a, \omega t_0) = (90^\circ, 60^\circ)$. Each line-to-ground voltage with the system frequency is plotted by a fine line. The line-to-ground voltage, for example, in phase *c* with an initial reignition abruptly changes from the instantaneous value to the trapped voltage just after the reignition, as shaded by vertical lines between the phase voltage and the trapped one in the figure. On the other hand, the transient variations in phases *a* and *b* initiate from the instantaneous value and build up to the first crest, as shaded by inclined lines between the phase voltage and the curve showing every first crest denoted by thick lines in the figure. Reignitions are expected to occur within the first increasing range of the recovery voltage in Fig. 2.13. Such range for phase *c* is just fully shown in Fig. 2.15. The variation for the line-to-ground voltage gives, in turn, the direct influence on the recovery voltage across the contacts, which is shown in Fig. 2.16 corresponding to Fig. 2.15. The expression is the same as Fig. 2.15. The magnitude of the voltage

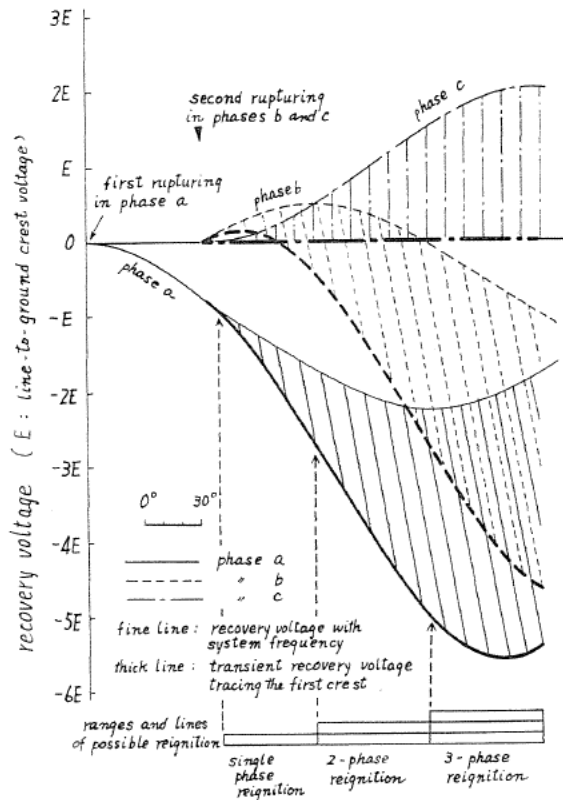


FIG. 2.16. Transient recovery voltage due to the initial reignition in phase *c*, when the steady state capacitive current is interrupted by the pattern of $\theta'_a = 90^\circ$, $t_0\omega = 60^\circ$.

across the contacts in phase c suddenly changes to nearly zero level at the moment of the reignition, and the voltage across the contacts in the other phases begin to build up steeply at the same time. Such transient recovery voltages often overtake the dielectric strength between the contacts. An induced reignition occasionally prevents the voltage transients from building up within the range of the shaded area, so that the line-to-ground voltage shown in Fig. 2.15 does not necessarily reach the crest value indicated by the thick line. This is one of the prominent characteristics in this field. The shaded domain in Fig. 2.15 or 2.16 indicates a limit for the line-to-ground overvoltage or the transient recovery voltage across the contacts. The characteristic tendencies of this overvoltage are as follows.

(1) The maximum transient component may be attained when a reignition occurs in phase a at $\theta'_a = 270^\circ$ in the pattern $(90^\circ, 90^\circ)$, but the maximum resultant line-to-ground overvoltage as high as $4.8E$ is induced in phase b with a reignition at $\theta'_a = 250^\circ$.

(2) The overvoltage is higher in the lagging phase than in the leading one with respect to the first reignited phase. But if a reignition occurs at the time when the recovery voltage begins to decrease, the overvoltage in the leading phase becomes higher.

(3) The transient component raises the line-to-ground voltage in the lagging phase, while it reduces in the leading one. In the latter case a remarkable high transient component happens to induce an overvoltage of the opposite polarity.

(4) The maximum overvoltage for each pattern is shown in Fig. 2.17. An overvoltage over $4E$ is always prospected in phase b , if the transient recovery voltage does not induce any reignition.

(5) The reignition at 180° after the previous extinction of arc does not always induce a highest overvoltage.

The characteristic tendencies for the voltage variation across the contacts are as follows.

(1) The maximum transient component as high as $6E$ may be attained when a reignition occurs in phase a at $\theta'_a = 270^\circ$ in the pattern $(90^\circ, 90^\circ)$.

(2) It is uncertain in which phase the transient voltage across the contacts becomes

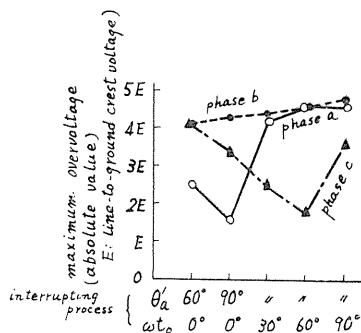


FIG. 2.17. Maximum overvoltage due to the initial reignition.

(3.2) Determination of possible reignitions

Transient variations of recovery voltage across the contacts due to an initial reignition often induce arcs in the other two phases. It is a new attempt to estimate the process of development of a reignition to the other phases under the following audacious assumptions, which may give a rather objective judgement.

(1) An initial reignition within the overlapped shaded area induces reignitions across the contacts in the other two phases, and results in a three-phase reignition. (cf. Fig. 2.16)

(2) An initial reignition within the separated shaded area induces a reignition in either phase, and results in a two-phase reignition. (*cf.* Fig. 2.16)

(3) The dielectric strength between the contacts in the first quenched phase is rather high in case of $\omega t_0 \neq 0$.

An example of the estimated range of the process is shown in the lower part of Fig. 2.16. The resultant estimated range for each pattern is shown in Table 2.6. The numerical results corresponding to Fig. 2.16 are arranged in the seventh row from the top. In actual cases, an initial reignition does not uniformly occur in all three phases, as shown in Table 2.2, and the time interval of ωt_0 is peculiar to each circuit breaker. Thus, the above-mentioned two factors must be considered when utilizing Table 2.6. Following two examples show the possibility of deducing theoretically the results of the "first reignition" in Table 2.3 from the data in Table 2.2 and 2.6.

TABLE 2.6. Estimated Range of Possible Reignition

Interrupting process		Line of initial reignition	Possible reignition		
θ'_a	ωt_0		3-phase reignition	2-phase reignition	Single phase reignition
90°	90°	<i>a</i>	60°	30° <i>c</i>	0°
		<i>b</i>	0°	140° <i>c</i>	20°
		<i>c</i>	80°	40° <i>b</i>	20°
		sum	140°	210°	40°
90°	60°	<i>a</i>	90°	30° <i>c</i>	0°
		<i>b</i>	0°	40° <i>c, a</i>	10°
		<i>c</i>	60°	60° <i>a</i>	50°
		sum	150°	130°	60°
90°	30°	<i>a</i>	70°	80° <i>b</i>	0°
		<i>b</i>	60°	20° <i>c, a</i>	0°
		<i>c</i>	60°	80° <i>a</i>	20°
		sum	190°	180°	20°
90°	0°	<i>a</i>	30°	120° <i>b</i>	0°
		<i>b</i>	80°	30° <i>c, a</i>	0°
		<i>c</i>	30°	20° <i>b</i>	0°
		sum	140°	170°	0°
60°	0°	<i>a</i>	0°	140° <i>b</i>	20°
		<i>b</i>	140°	0°	0°
		<i>c</i>	60°	20° <i>b</i>	0°
		sum	200°	160°	20°
Total			820°	850°	140°

Ex. 1. Test results of Kakomachi SS

Since each interruption follows the process of $(\theta'_a, \omega t_0) = (90^\circ, 68^\circ)$ as average, the rows of $(90^\circ, 60^\circ)$ in Table 2.6 are available to determinate the types of the possible reignition. From Table 2.2, the initial reignition of Type I-b occurs in

the following ratio; phase a : phase b : phase $c = 2 : 1 : 2$. Thus, the effectively estimated range for the reignition over three lines is

$$90^\circ + 60^\circ = 150^\circ \dots\dots\dots 48\%,$$

the effectively estimated range for the reignition over two lines is

$$30^\circ + 40^\circ \times 0.5 + 60^\circ = 110^\circ \dots\dots 35\%,$$

the effectively estimated range for the reignition in a single line is

$$10^\circ \times 0.5 + 50^\circ = 55^\circ \dots\dots\dots 17\%.$$

The actual numbers of each type are 4, 0 and 2 from the row for Type I-b in Table 2.3, respectively. The fact that the reignition over three lines is most likely to be induced may be derived from the above estimation.

Ex. 2. Test results of Kasumori SS

Since each interruption process falls within $\theta'_a = 70^\circ$ to 80° , and $\omega t_0 = 0^\circ$ to 30° , the data must be treated under the consideration of the following three processes at a time: $(\theta'_a, \omega t_0) = (90^\circ, 30^\circ)$, $(90^\circ, 0^\circ)$ and $(60^\circ, 0^\circ)$. From Table 2.2, the initial reignition of Type I-b occurs in the following ratio, phase a : phase b : phase $c = 1 : 10 : 2$. Thus, the effectively estimated range for the reignition over three lines is

$$\left. \begin{array}{ll} \text{for phase } a & (70^\circ + 30^\circ + 0^\circ) \times (1/13) = 8^\circ \\ \text{for phase } b & (60^\circ + 80^\circ + 140^\circ) \times (10/13) = 215^\circ \\ \text{for phase } c & (60^\circ + 30^\circ + 60^\circ) \times (2/13) = 23^\circ \end{array} \right\} \text{ total } 246^\circ \dots\dots 73\%,$$

the effectively estimated range for the reignition over two lines is

$$\left. \begin{array}{ll} \text{for phase } a & (80^\circ + 120^\circ + 140^\circ) \times (1/13) = 26^\circ \\ \text{for phase } b & (20^\circ + 30^\circ + 0^\circ) \times (10/13) = 39^\circ \\ \text{for phase } c & (80^\circ + 20^\circ + 20^\circ) \times (2/13) = 19^\circ \end{array} \right\} \text{ total } 84^\circ \dots\dots 25\%,$$

the effectively estimated range for the reignition in a single line is

$$\left. \begin{array}{ll} \text{for phase } a & 20^\circ \times (1/13) = 2^\circ \\ \text{for phase } b & 0^\circ \times (10/13) = 0^\circ \\ \text{for phase } c & 20^\circ \times (2/13) = 3^\circ \end{array} \right\} \text{ total } 5^\circ \dots\dots\dots 2\%.$$

The actual numbers of each type are 10, 7 and 0 from the row for Type I-b in Table 2.3, respectively. This estimation is rather satisfactory.

These two examples show that the estimation on the bases of Table 2.6 may lead to the actual tendency.

(3.3) Reignition over two or three lines

The limit of the overvoltage due to the free oscillation after the reignition over two or three lines will be investigated with the same procedure as the previous section. The circuit condition with the capacitance C connected in parallel with either of C_s 's in Fig. 2.14 may be regarded as that corresponding

to the reignition over two lines. Since the initial voltages across these two capacitances are uniquely given by the voltages trapped on the lines, the transient wave form does not depend on the sequence of the initiation of reignitions but on the combination of two lines. The original equations in (3.5) may also be available for this case. Initiated by the reignition over two lines, each free oscillation generally builds up from each trapped voltage to the first crest with the cosine-like wave front. The first crests of these oscillations are given as follows.

$$E_{c1 \max} = \frac{\sqrt{3}}{2} E \sqrt{1+k^2+2k \cos \theta_f} \sin\left(\theta'_1 + \frac{\pi}{6} + \chi'\right) - \frac{k}{2}(E_{01} + E_{02}) + \frac{1}{2}(E_{01} - E_{02}), \quad (8.1)$$

$$E_{c2 \max} = \frac{\sqrt{3}}{2} E \sqrt{1+k^2+2k \cos \theta_f} \sin\left(\theta'_1 + \frac{\pi}{6} + \chi'\right) - \frac{k}{2}(E_{01} + E_{02}) - \frac{1}{2}(E_{01} - E_{02}), \quad (8.2)$$

where $\tan \chi' = \frac{\sin \theta_f}{\cos \theta_f + k}$, and suffixes, 1 and 2, discriminate the two lines following the positive phase sequence, E_{01} and E_{02} are the trapped voltages on the both lines, θ'_1 is the electrical angle of the phase voltage at the instant of reignition as to the line with the suffix 1, and $\theta_f = \omega \cdot \pi / \nu$. Eqs. (8) indicate that both transient voltages, E_{c1} and E_{c2} oscillate symmetrically with the DC component, shown in the third terms of Eqs. (8), as a shifted center. Fig. 2.18 is an example of a reignition over phases a and c with 400 c/s as a typical free oscillating frequency. The first crest is realized after $1/2$ period of 400 c/s, that is, after $\theta'_f = 27^\circ$ for

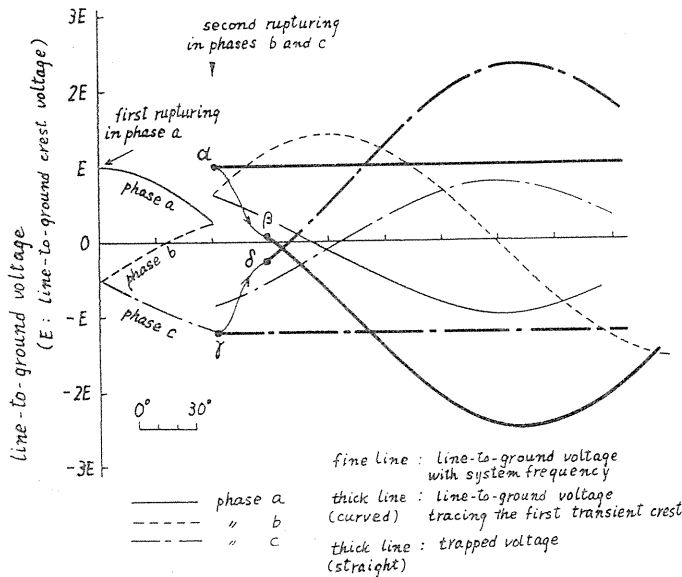


FIG. 2.18. Line-to-ground overvoltage due to a reignition over phases a and c , when the steady state capacitive current is interrupted by the pattern of $\theta'_a = 90^\circ$, $\omega t_0 = 60^\circ$.

the electrical angles of the system frequency since the instant of reignition. Eqs. (8) are plotted against θ'_1 in Fig. 2.18 by a thick line. For example, in a reignition over phases a and c just after the second rupturing, two free transient oscillations initiate from the point " α " and " γ ", which are equal to the voltages initially trapped on the lines in phases a and c , and build up to the point " β " and " δ ", respectively. The curve between " α " and " β ", or " γ " and " δ " are nothing but the first wave front. Fig. 2.20 shows the maximum overvoltages

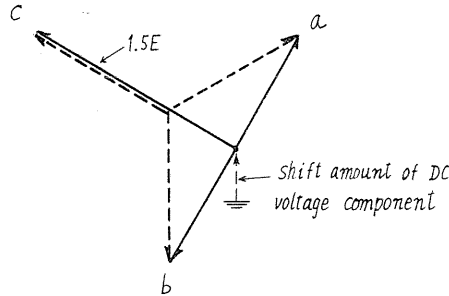


FIG. 2.19. Vector diagram during a reignition over two lines.

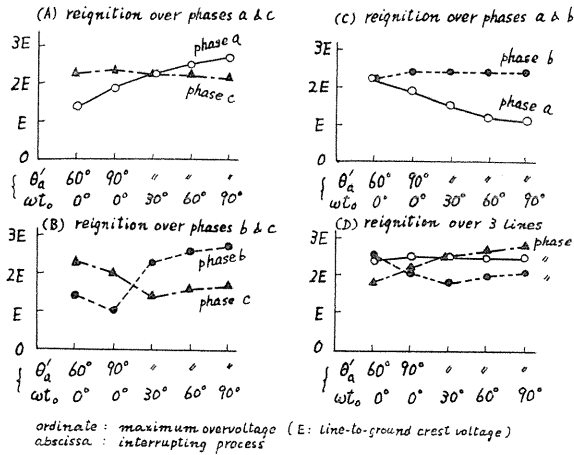


FIG. 2.20. Maximum overvoltage due to a reignition over two and three lines.

considered for every combination. These crests are always realized if a reignition once occurs. This is a feature of this transient. The line-to-ground voltage in an unignited phase continues to oscillate with " $1.5E$ " vector as the center pointed out in Fig. 2.19. Since the shift amount of DC voltage component during this reignition is lower than that during an initial reignition, this new voltage transient does not generally magnify the previous transient peak. In an example of Fig. 2.10(a), the voltage transient in phase B initiates to oscillate to the opposite direction from the mid-point of the first oscillation just after the time t_1 when two arcs are reignited in phase R and W at the same time.

Next, in a reignition over three lines, it is a feature that the neutral potential during the transient oscillation has no shift of DC component. A transient oscil-

lation in each line initiates from each trapped voltage and oscillates with the normal phase voltage as the center. The first maximum crest is given as the equation

$$E_{ck \max} = E\sqrt{1+k^2+2k\cos\theta_f'}\sin(\theta_k'+\gamma') - E_{0k}, \quad (9)$$

where κ may be a , b or c , θ_k' is the electrical angle of each phase voltage and other constants are the same as those in Eqs. (8). Fig. 2.21 is an example with 400 c/s as a typical oscillating frequency. Fig. 2.20(d) shows the maximum overvoltages for each case, which amount to nearly the same values as in the reignition over two lines. When a reignition is once initiated, these maxima are always realized in this case, too.

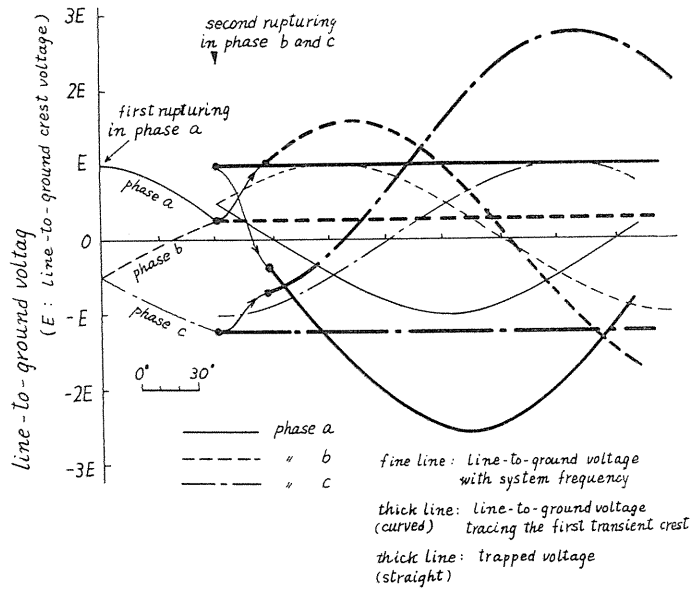


FIG. 2.21. Line-to-ground overvoltage due to a reignition over three lines when the steady state capacitive current is interrupted by the pattern of $\theta_a' = 90^\circ$, $\omega t_0 = 60^\circ$.

(3.4) Line-to-line overvoltages

When a reignition over two lines is caused during an interrupting process, the crests of the line-to-ground voltage transients are given by Eqs. (8) in (3.3). The neutral potential-to-ground of this transient has a shift of DC component which is equal to the average value of both trapped voltages in two lines concerned and the voltage loci of these oscillating components are symmetrical to this shifted value. Therefore, twice the amount of this component is to be impressed on the insulations between two lines. This line-to-line component can be derived from Eqs. (8.1) and (8.2) with the consideration of the supposed direction for each voltage,

$$\begin{aligned}
 E_{12 \max} &= E_{c1 \max} + E_{c2 \max} \\
 &= \sqrt{3} E \sqrt{1+k^2+2k \cos \theta_f} \sin\left(\theta'_1 + \frac{\pi}{6} + \lambda'\right) - k(E_{01} + E_{02}). \quad (10)
 \end{aligned}$$

Next, Eq. (9) gives the first crest during a reignition over three lines. At that instant the voltage impressed between two lines can be given by the equation

$$\begin{aligned}
 E_{12 \max} &= E_{c1 \max} - E_{c2 \max} \\
 &= \sqrt{3} E \sqrt{1+k^2+2k \cos \theta_f} \sin\left(\theta'_1 + \frac{\pi}{6} + \lambda'\right) - k(E_{01} - E_{02}). \quad (11)
 \end{aligned}$$

In each of both Eqs. (10) and (11), the first term is the same and in the second term, the signs are different in the parenthesis. But these two equations are quite equal, because the supposed positive direction of each voltage is essentially taken in the opposite side.

Thus, the first crest voltage impressed on between two lines is always the same in both cases of reignition over two lines and over three lines. Fig. 2.22 shows the numerical solution of Eq. (9) or (10) plotted against θ'_1 as a variable.

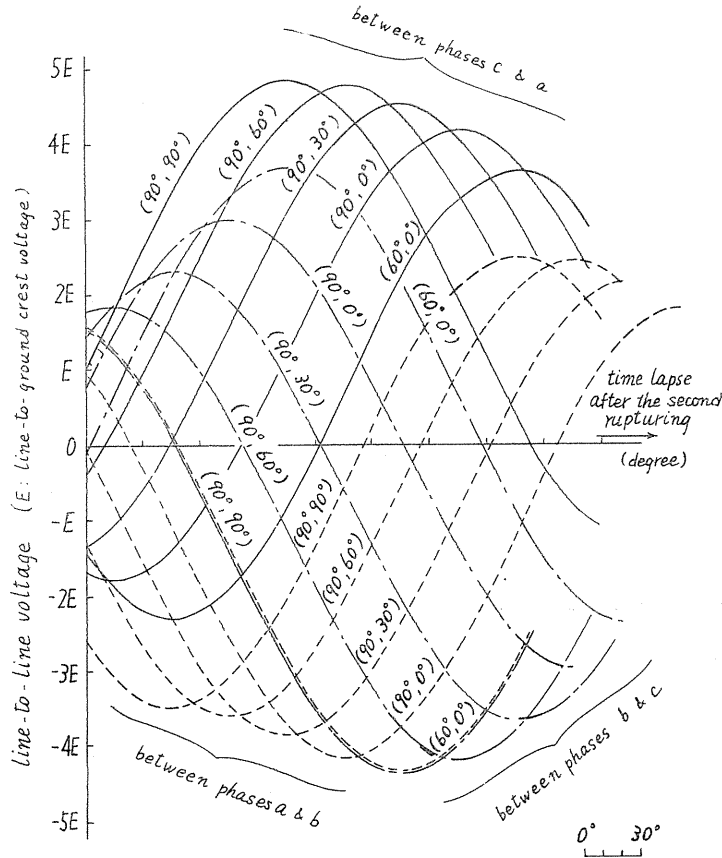


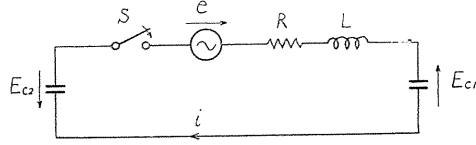
FIG. 2.22. Line-to-line overvoltage during a reignition over two or three lines.

The origin of this figure is taken from the initial point of the second rupturing. The parameters on these curves are selected as to correspond to the typical interrupting patterns mentioned before.

(3.5) Original equations

The followings are the original equations which lead to the Eqs. (2) to (11). Fig. 2.23 is a series circuit consisting of the four circuit elements, L , R , C_1 and C_2 . For the analyses of transient voltages in power systems, it is more convenient to make use of the oscillating frequency and the damping factor as the parameters in stead of the formal circuit constants. Thus, the following equations can be derived, where $\alpha = C_1/C_2$, ν_1 is the resonant frequency derived from by L , R , C_1 and C_2 and Q_1 is a quality factor for its series resonance. The source voltage is $e = e_m \sin(\omega t + \theta)$, where ω is the system angular frequency and θ is the reignited phase angle. The initial conditions are $E_{c1} = E_{01}$, $E_{c2} = E_{02}$ and $i = 0$ at $t = 0$.

FIG. 2.23. L - C - R series circuit.



$$i = \frac{\alpha C_1 e_m}{(1 + \alpha) \sqrt{\gamma}} \left\{ \omega \sin(\omega t + \theta + \phi_1) + \nu_1 A \varepsilon^{-t/\tau_1} \sin(\nu t + \xi_1) \right\} - \frac{\alpha \nu_1 C_1 (E_{01} + E_{02})}{(1 + \alpha) \sqrt{1 - 1/4 Q_1^2}} \varepsilon^{-t/\tau_1} \sin \nu t$$

$$E_{c1} = \frac{\alpha e_m}{(1 + \alpha) \sqrt{\gamma}} \left\{ -\cos(\omega t + \theta + \phi_1) - A \varepsilon^{-t/\tau_1} \sin(\nu t + \xi_1 + \varphi_1) \right\} - \frac{\alpha (E_{01} + E_{02})}{1 + \alpha} \left\{ 1 - \frac{1}{\sqrt{1 - 1/4 Q_1^2}} \varepsilon^{-t/\tau_1} \sin(\nu t + \varphi_1) \right\} + E_{01}$$

$$E_{c2} = \frac{e_m}{(1 + \alpha) \sqrt{\gamma}} \left\{ -\cos(\omega t + \theta + \phi_1) - A \varepsilon^{-t/\tau_1} \sin(\nu t + \xi_1 + \varphi_1) \right\} - \frac{E_{01} + E_{02}}{1 + \alpha} \left\{ 1 - \frac{1}{\sqrt{1 - 1/4 Q_1^2}} \varepsilon^{-t/\tau_1} \sin(\nu t + \varphi_1) \right\} + E_{02}$$

where

$$\nu = \nu_1 \sqrt{1 - \frac{1}{4 Q_1^2}}, \quad \tau_1 = \frac{2 Q_1}{\nu_1}$$

$$A = \sqrt{\frac{1}{1 - 1/4 Q_1^2} \left(\frac{\omega}{\nu_1} \cos \theta - \frac{1}{2 Q_1} \sin \theta \right)^2 + \sin^2 \theta}$$

$$\gamma = \left(1 - \frac{\omega^2}{\nu_1^2} \right)^2 + \left(\frac{\omega}{Q_1 \nu_1} \right)^2$$

$$\tan \phi_1 = Q_1 \left(\frac{\nu_1}{\omega} - \frac{\omega}{\nu_1} \right)$$

$$\tan \varphi_1 = \sqrt{4 Q_1^2 - 1}$$

$$\tan \xi_1 = \frac{\omega}{\nu_1} \sqrt{1 - \frac{1}{4 Q_1^2}} \cdot \frac{1 - \frac{\omega^2}{\nu_1^2} + \frac{\omega}{Q_1 \nu_1} \tan \theta}{\frac{\omega}{2 Q_1 \nu_1} \left(1 + \frac{\omega^2}{\nu_1^2} \right) - \left\{ 1 + \frac{\omega^2}{\nu_1^2} \left(\frac{1}{2 Q_1^2} - 1 \right) \right\} \tan \theta}$$

Chapter 3. Interruption of Small Inductive Current with Current Chopping

§ 1. Current interruption of unloaded transformers

There are two sorts of method to interrupt the transformer magnetizing current; one is the interruption of the steady state magnetizing current and the other is that of the inrush current with asymmetrical components. In the recent experiments in actual systems the current chopping was generally caused by air-blast circuit breakers, while it was never caused by oil circuit breakers or porcelain type circuit breakers which seldom impress the overvoltages in the system. After an arc extinction, any trapped voltage does not leave on transformer terminals as was experienced in case of the de-energization of capacitive circuit, and the resulting recovery voltage across the contacts is relatively low. At the moment of the arc extinction at the normal current zero passage, any overvoltage would never occur on the de-energized transformer terminals. In an air-blast circuit breaker, air flow with elevated pressure and high velocity tries to quench an arc at the instant of the contact separation and consequently the current form turns out irregular. With the current rupturing at other than a normal zero passage, the transient voltage may appear across the transformer terminals. That transient also results in a rapid building up of the voltage across the switch contacts, which may, in turn, cause an arc reignition, if the transient recovery voltage overtakes the dielectric strength of the opening contacts. A number of restriking may actually occur in succession. The wave shape of the voltage looks like the saw-toothed form and the current fluctuates violently. During such successive restriking period the peak values of the current gradually decrease and each of the instantaneous chopped values also becomes lower, while the dielectric strength across the opening contacts becomes higher, so that the final rupturing is achieved at last. Fig. 3.1(a) is a typical oscillogram showing the interruption

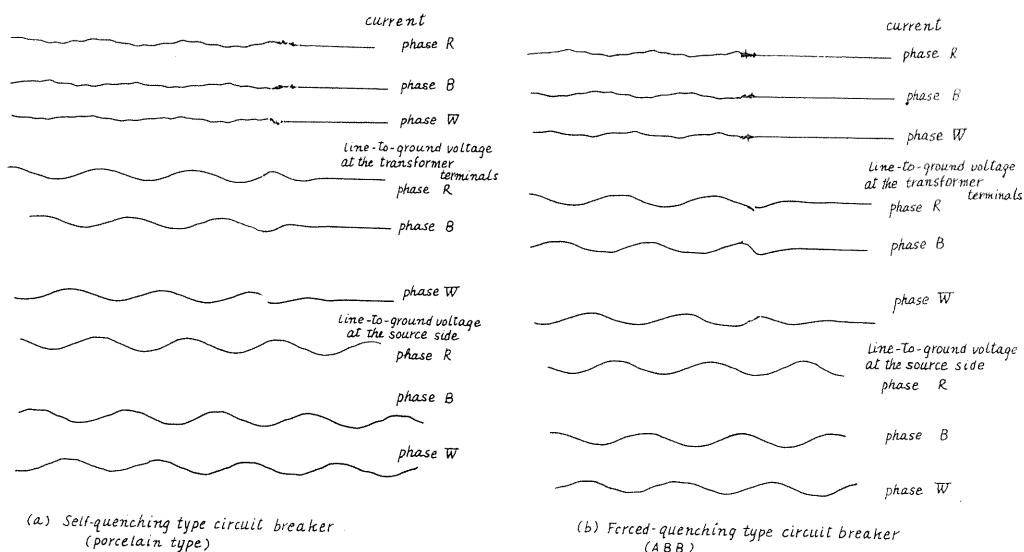


FIG. 3.1. Interruption of steady state magnetizing current of an unloaded transformer.

of the steady state magnetizing current by a procelain type circuit breaker and Fig. 3.1(b) is one by an air-blast circuit breaker. Phenomena in a close-open-test (CO-test in brief) will be discussed in the following sections. A CO-test gives a characteristic wave shape of the current ruptured, which is generally a symmetric and consists of the two repeating parts, one with the value sufficiently large as comparable with the rated current and the other so small as that of the normal magnetizing current. Since these two singular parts are repeated alternately, the course of the current interruption takes various processes, depending upon the time when the contacts begin to separate. Fig. 3.2 (a) is the case of the contact separation in the lower current period, and Fig. 3.2(b) is in the higher current period.

In order to research the frequency of occurrence of overvoltages affected by the environmental factors, the interrupting phenomena in these CO-tests are fully discussed.

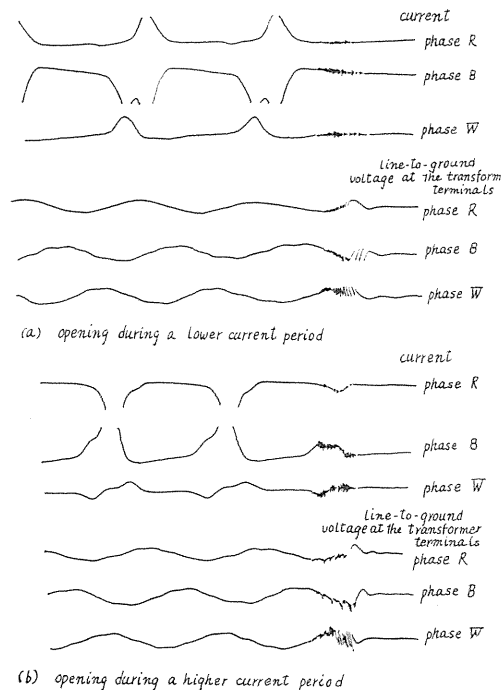


FIG. 3.2. Interruption of inrush magnetizing current of an unloaded transformer by air-blast circuit breaker.

§ 2. Overvoltages and “off-peak current ratio”

On energizing a three-phase unloaded transformer with isolated neutral, the magnetic flux fluctuates by proper instantaneous amount, depending on the phase angle at the instant when the voltage is supplied. If the magnetic saturation be disregarded, the magnetizing current would also fluctuate similarly, keeping the normal 120° phase difference such as in the steady state.³¹⁾ But, in practice, the maximum value of the fluctuated flux becomes much more than the rated amount and reaches the saturated region of the iron core, so that the current magnitude for this region develops up to a few multiple of the rated current, and the wave shape of the current becomes quite different from the sinusoidal form.

In general the normal magnetizing current contains the higher harmonics when energized by the sinusoidal source, by the effect of the magnetic characteristics. These harmonics often raise some disturbances on the power systems. Some devices to compensate or suppress the harmonics were discussed. It is impossible to eliminate the harmonics by the mere method of taking the rated flux level lower. The complete elimination is accomplished by means of whether the suitable connection of the windings or the elaborated core construction. The series of 3rd, 9th harmonics is eliminated rather easily, but complicate devices are necessary to suppress the series of 5th, 7th harmonics.³²⁾ Buch and Heuter provided a tertiary winding with a suitable reactance³³⁾ and Biermann

designed a special core with slots.³⁴⁾ The transformer with such improvements results in the raise of cost, the complicated construction and, rather, the shortage of reliability, so that such designs have rarely been adopted.

Even such improved transformer could be accompanied with the inrush magnetizing current. The initial impedance, on which the current depends during the inrush period, is nearly equal to that of the winding itself without core, and it has little relation to the above-mentioned transformer construction. The informations on the inrush current have been found since the beginning of this century,³⁵⁾ and those phenomena have been discussed³⁶⁾. Many papers are published still now, for example, on the comparison between the inrush current and the short circuit current³⁷⁾, on the estimation of the decay of the current with time³⁸⁾, and on the influences of the inrush current on the system operation³⁹⁾⁴⁰⁾. All these papers, however, mainly dealt with the peak value of the inrush current, and few papers dealt with the current wave form itself, and consequently they cannot be available for this discussion on the interrupting phenomena under CO-test. Figs. 3.3(a) and (b) show typical examples of the inrush current of an unloaded transformer. One cycle consists of two parts: the higher and the lower current periods. During the lower current period, the magnetic flux in the core may be within the unsaturated region, and the current increases gradually as the flux density approaches the knee of the characteristic curve. The current of each line in Fig. 3.3(a) has a form resembling to the rectified-half wave, *i.e.* a completely asymmetrical form, but in Fig. 3.3(b) the current of phase *W* has lower peaks, and has a nearly symmetric form. The former wave shape takes place when a phase voltage is fed at or near its zero passage, while the latter one when at or near its crest. Taking these two forms as both extremes, other wave shapes of inrush current show some mixed forms of them according to the switching chances.

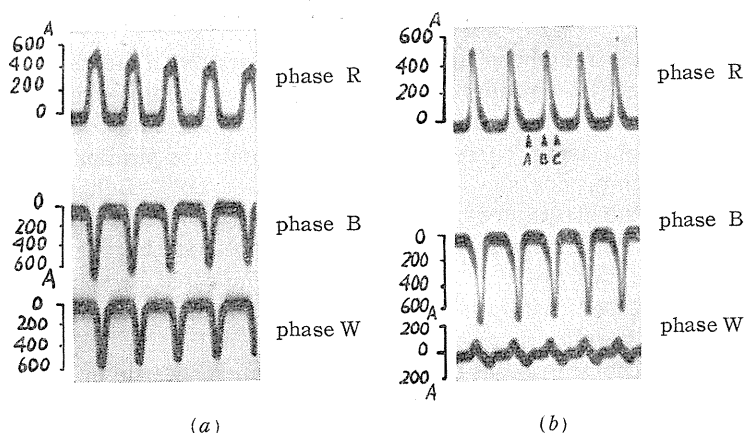


FIG. 3.3. Typical inrush current forms of unloaded three-phase transformer (60 MVA, 154/77 KV).

As shown in Fig. 3.3(b), if the separation of the contacts begins at a point *A* during the lower current period in phase *R*, the powerful air stream may quench an arc and realize the final rupturing at once. Since the magnetic flux,

in this period, is lower than the knee-value, the crest of the voltage transient does not become high even in case of the current chopping. If their separation begins at a point *B* during the higher current period, the arc energy is prominent and it prevents the breaker from quenching and, therefore, the final rupturing is postponed to near the point *C* where the rush current comes back to the lower magnitude. After such prolonged time interval, however, the switch contacts come to separate over an adequate distance so that the air flow can easily quench the burning arc. As the result of such condition, the instantaneous value of the chopped current may be come higher, and the corresponding released magnetic energy may be greater than that of the former case. Thus, the transient peak may reach to rather higher crest.

Now, on trial, the following ratio is defined to represent a degree of skewness in the current form.

$$\text{the "off-peak current ratio"} = \frac{\text{the period carrying lower current}}{\text{the period of one cycle}}$$

The larger this ratio is, the shorter the rush period is, and the smaller is the possibility that the contacts happen to open in the higher current period. Even if the quenching process is finished during that period, rush current only flows for a short time, so that, the instantaneous magnitude of chopped current will be lower and a resultant crest will be the same. When this ratio is small, all the condition becomes contrary. From such point of view, oscillograms obtained in the test series of Table 1.1 are investigated. The results are shown in Figs. 3.4(a) to (e). The notations, for example, "Yamaguchi D-1", "Tamagawa D-2" and so on, are those of the circuit breakers. In Fig. 3.4 the overvoltage on each transformer terminal is plotted against the off-peak current ratio, the former on the ordinate and the latter on the abscissa. The lower current period is obtained from the oscillograms. Every current is measured through a current transformer (CT) and, therefore, the DC component is not correctly transferred to the secondary side and the true zero level is biased on the oscillograms. It is only true, however, that the flat part of every inrush current carries lower value. Accordingly, an intersection point of the flat part with the tangent at the point of inflexion on the mid slope of rush current is equivalently regarded as the boundary between both periods, as shown in Fig. 3.5.

More detailed investigations of oscillograms indicate that the inrush currents in three lines reach to excessive values nearly at the same time and lose the phase difference of 120° between lines as is the case with the stationary state. Thus, in Figs. 3.6(a) to (e) is plotted the maximum overvoltage produced in a single test against the off-peak current ratio for the common lower current period in three lines.

In Figs. 3.4 and 3.6, the upper limits of prospective overvoltages are shown by the chain lines. Fig. 3.7 collectively represents all such curves that decrease monotonously as the off-peak current ratio increases, that is, the shorter the lower current period is, the higher the upper limit is. A curve is plotted in case of a porcelain type circuit breaker denoted by "Tamagawa D-4" as a reference. It does not depend upon the off-peak current ratio. Not only "Tamagawa D-4" but other self-quenching circuit breakers have no ability to chop the current and interrupt the magnetizing current without remarkable overvoltage.

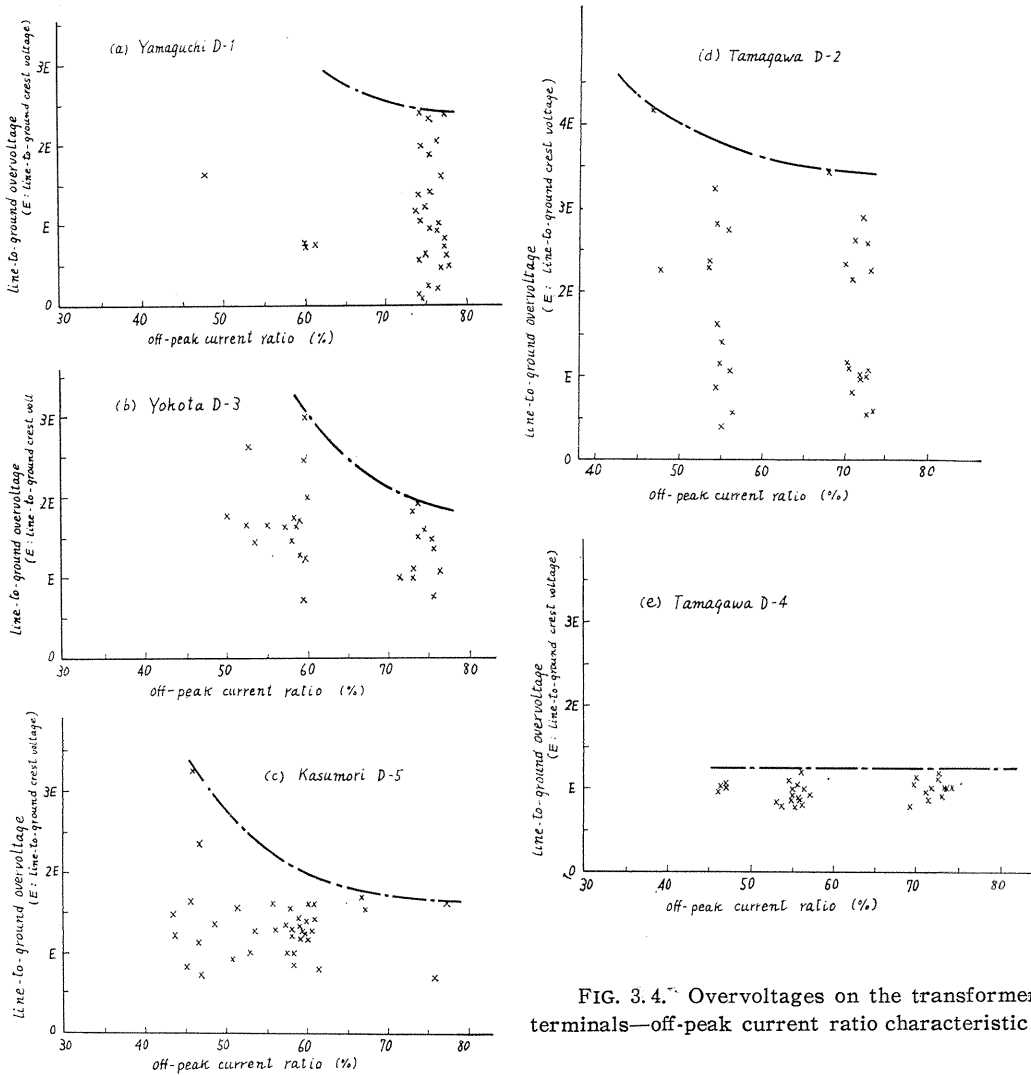


FIG. 3.4. Overvoltages on the transformer terminals—off-peak current ratio characteristic.

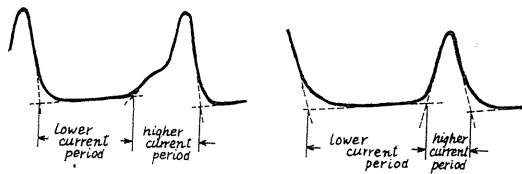


FIG. 3.5. Discrimination of higher and lower current periods.

Then, Fig. 3.8 shows the frequency of occurrence of the off-peak current ratio in each line, which concentrates between 40 and 70%. In "Yamaguchi D-1", 66.7% of the whole tests showed nearly the same wave form whose off-peak current ratio was 75%. It is wondered if any other factors gave influences. This

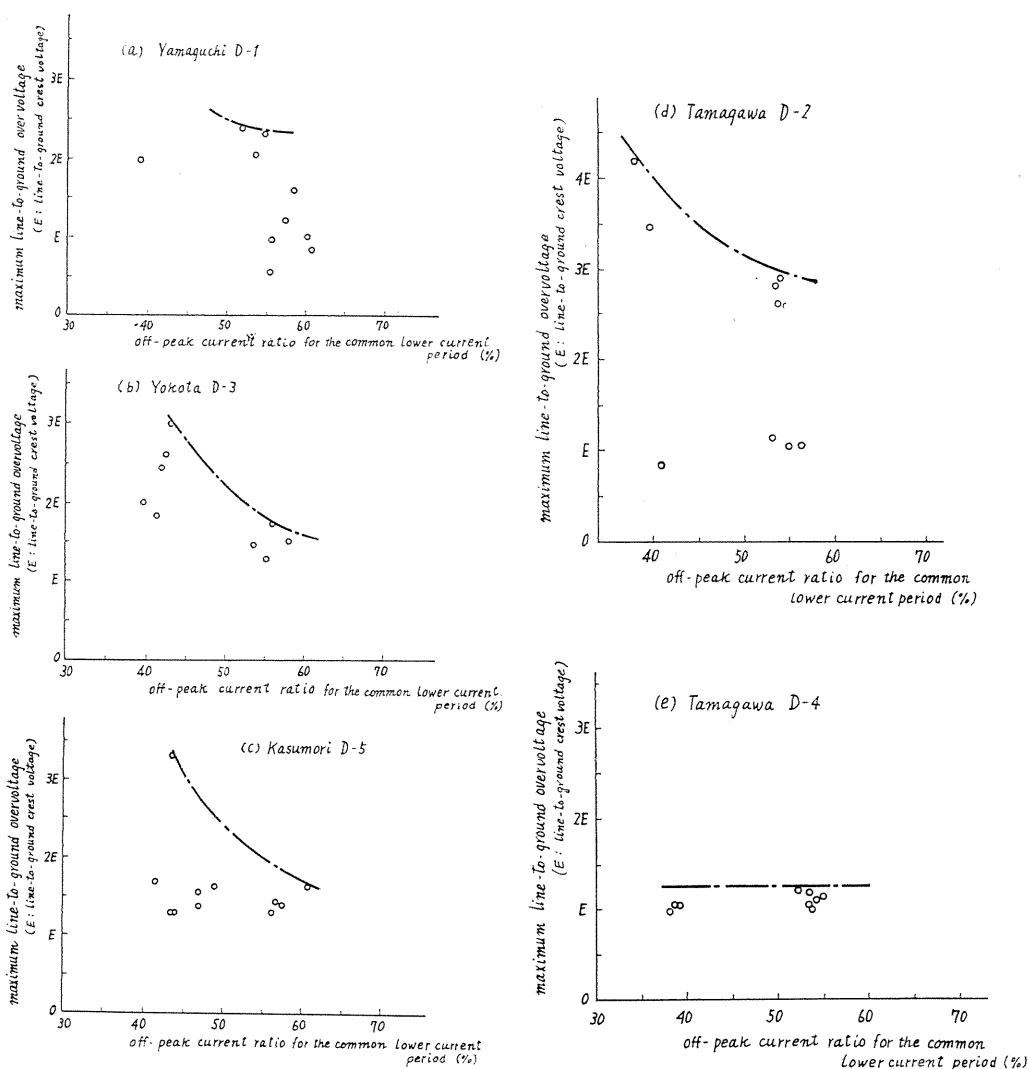


FIG. 3.6. Maximum overvoltages in three lines on the transformer terminals—common off-peak current ratio characteristic.

ratio in the common period in three lines is rather reduced in value than the off-peak current ratio in each line.

§ 3. Overvoltages and “prospective charge” to be interrupted

It is only apparent in the previous section that the upper limit of the overvoltages depends upon the off-peak current ratio. But various overvoltages are found on a vertical line corresponding to the same ratio. If a series of phenomena from the separation of contacts to the final rupturing is all accomplished in a short period of lower current, the excessive transient overvoltage cannot build up. In a certain condition of given circuit and breaker, the factors which

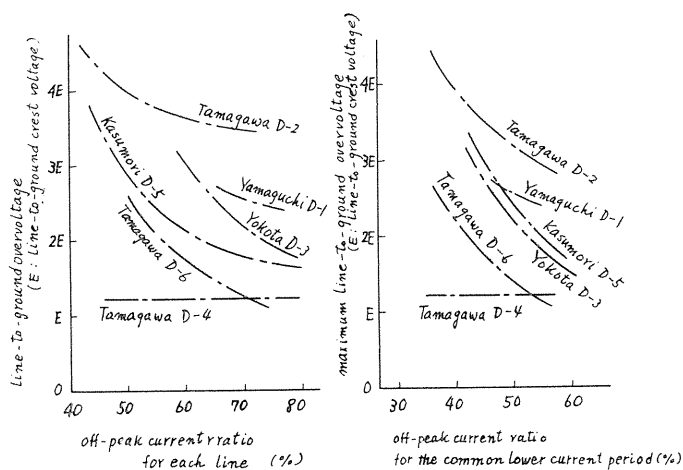


FIG. 3.7. Upper limits of prospective overvoltages.

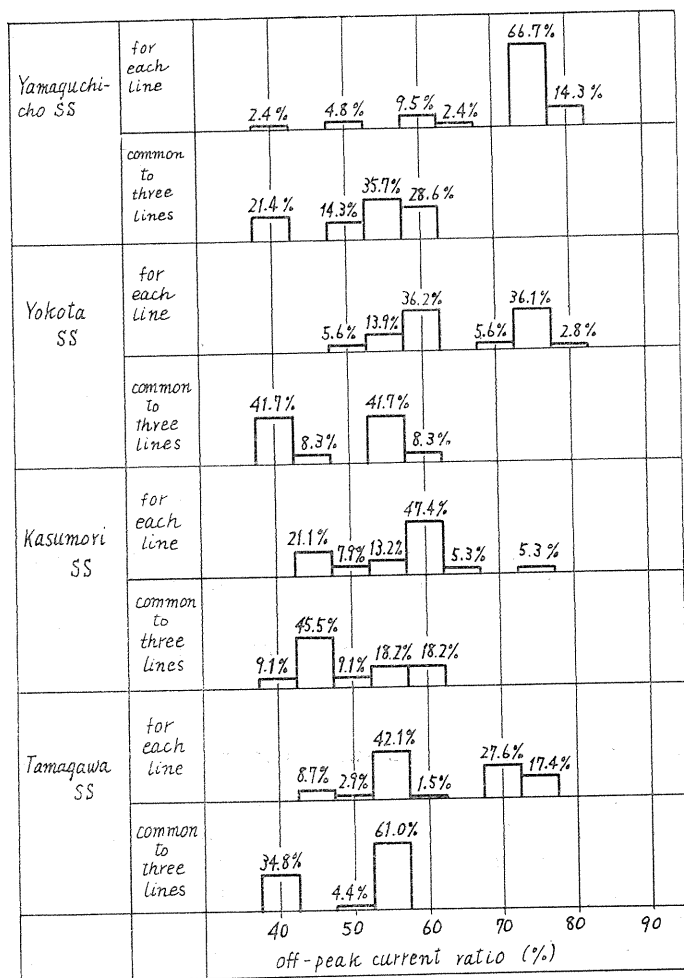


FIG. 3.8. Frequency of occurrence of lower current period.

give influences on the crest of the voltage transient after chopping consists of the following two; one is the current which is expected to flow after the separation of the contacts, and the other is the period between the separation of the contacts and the final rupturing. Thus, a product of both amounts may be considered as a new variable, and oscillograms again investigated from such a new point of view.

The time, when the contacts begin to separate, is introduced to this estimation as an important factor. The separation of the contacts is caused quite at random during a cycle. Provided that a current wave form and a time when the contacts begin to separate are given, the current i and the period t for the shaded area in Fig. 3.9 should be considered as the two factors concerned. Then, the time integration of i during t is calculated for this shaded area, and it has a dimension of the electric charge.

The current during the arcing period after the separation of the contacts is different from the previous form supposing the contact does not separate. Moreover, every wave form is quite different in every test even under the same external conditions. The actual current flowing through the arc is considered as the result of the difference between the diverged energy from arc and the quenching energy of air flow. The true severity imposed on the space between the contacts must be given by the current expected to flow as before. Besides, it is clarified by several trials that overvoltages are more closely connected with the integration of the current before the separation. As the actual procedure, the point A, at which the contacts begin to separate, is found on an oscillogram at first, as indicated in Fig. 3.10.

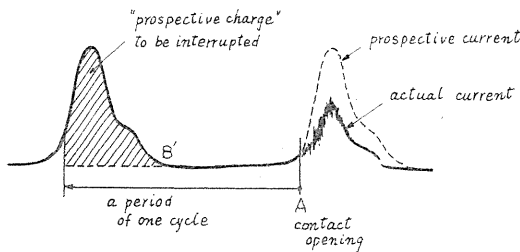


Fig. 3.10. Definition of "prospective charge".

Relations between the overvoltages and the prospective charge are shown in Figs. 3.11 (a) to (e) for each line, and in Figs. 3.12 (a) to (e) for each test. The abscissa of the latter diagrams represents the summation of the prospective charges in all the three lines and the ordinate shows the maximum overvoltage observed in a single test. The abscissa is graduated by $Q(\text{coulomb}) = (\text{amp}) \times (\text{sec})$, if a current is numerically defined, otherwise it is graduated by an arbitrary quantities. Since the graduation of the abscissa is logarithmic, each curve may be displaced horizontally with necessary amounts without any deformation of the shape itself, thus all the diagrams are theoretically compared with

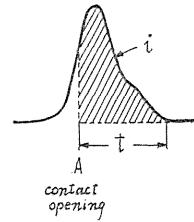


FIG. 3.9. Current wave form after the contacts open.

indicated in Fig. 3.10. The current is integrated from the point just before one cycle of the point A to the time B' when the current reduces to nearly zero. That integration corresponds to the shaded area in Fig. 3.10. That area is briefly called as the "prospective charge" to be interrupted in the following discussion. The area is practically considered as null when the separation begins in the lower current

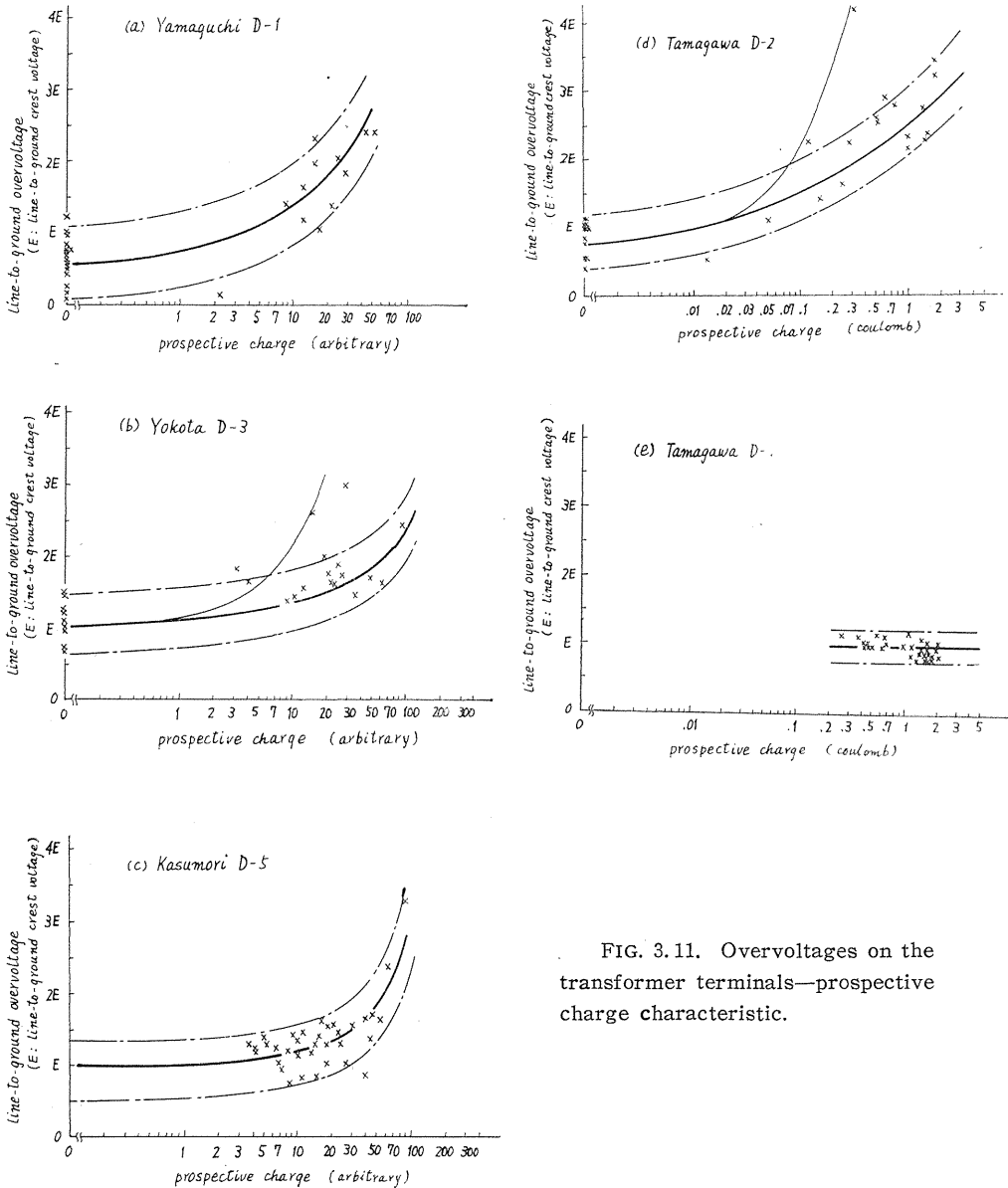


FIG. 3.11. Overvoltages on the transformer terminals—prospective charge characteristic.

each other for the same purpose.

The use of this prospective charge offers several advantages. Some circuit breakers may cause successive restriking during the quenching period even if the contacts separate within the lower current period, by the reason that the recovery rate of dielectric strength is slower than the building up of the transient recovery voltage. In such case, every chopped current is kept in lower value and every crest of transients does not reach to higher level, although the quench-

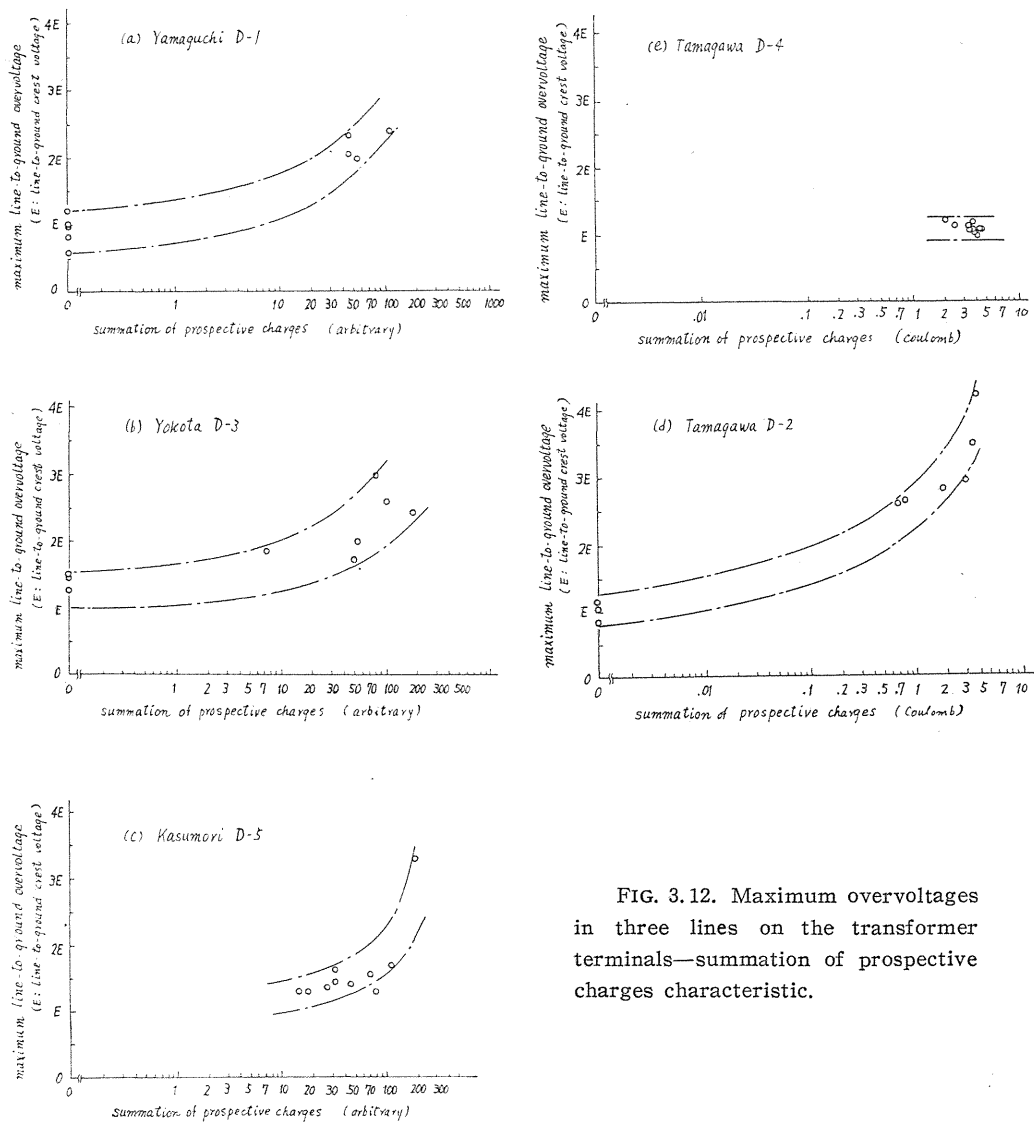
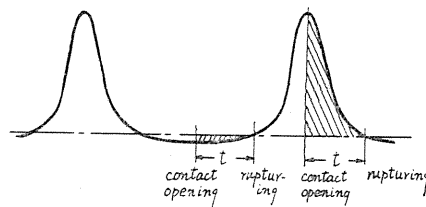


FIG. 3.12. Maximum overvoltages in three lines on the transformer terminals—summation of prospective charges characteristic.

FIG. 13.13. Difference of prospective charge depending on the opening chance.



ing process requires comparatively a long time. On the contrary, when the separation of the contacts begins just before the inrush period, the final rupture is postponed until the inrush period is over and the current comes back to near

zero level again. In this case, the instantaneous magnitude of the chopped current may be larger and the transient crest may reach to higher level. Accordingly, if these two transient crests are plotted against the quenching time required, two points must be arranged on the same quenching time and an unique relation cannot be obtained. But, as shown in Fig. 3.13, the prospective charge takes lower amount for the former case and higher for the latter. In case where the inrush current may be suppressed by the quenching action, the chopped current and the transient crest are apt to reach to a considerably high level. If the integration is carried out for the actual current, the prospective charge calculated will become rather small and, therefore, the result is plotted on the ordinate near the left side of the chart. Since the points for the lower current period are plotted against the same integrated value, this does not also result in an unique relation. All the points in two cases, above-mentioned, should be plotted on the respective position for the strictly defined prospective charge.

Every curve in Figs. 3.11 and 3.12 increases monotoneously. The reason, why these diagrams apparently have less points corresponding to lower prospective charge, is that the lower integrated values are always regarded as zero when the separation and the rupturing are achieved within a lower current period. Every diagram is shown with the fluctuation of $\pm 0.5 E$ around the solid curve. Such fluctuations are caused not only by the irregularity of air flow, the instability of arc burning in air stream, but also by the variety of peak value of every inrush current. The comparison of many inrush current for the same transformer reveals that the peak magnitudes among the similar wave forms are not necessarily equal. The previous residual magnetic flux in the core may have some influences on such unequality.

In Fig. 3.11, plotted for each line, the overvoltages up to 3 to 4 times the normal line-to-neutral crest are sometimes caused for the prospective charge of the moderate value in some circuit breakers, for example, in "Tamagawa D-2".

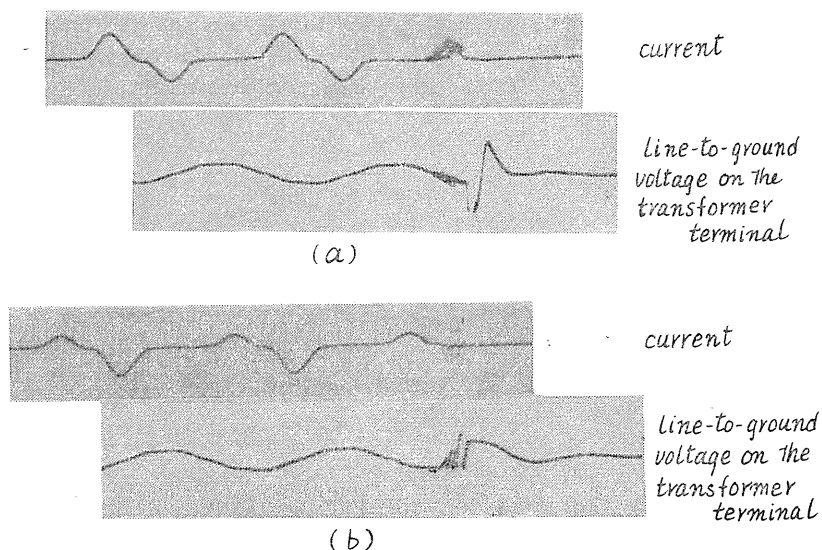


FIG. 3.14. Singular examples.

The current in Figs. 3.14(a) and (b), corresponding to such cases, has a small positive and negative peak with a similar amount, and has zero passage between them which just corresponds to the crest of the phase voltage. If such a current is chopped before the zero passage, the transient oscillation is so produced as to elevate the normal crest voltage and leads to an extremely high overvoltage, as shown in Fig. 3.14(a). On the contrary, if chopped after the zero passage, the transient oscillation brings down the normal crest, as shown in Fig. 3.14(b). These two oscillograms were obtained at the 7th and the 10th records out of a series of 10 times experiments. A small difference of the rupturing point causes the transient oscillation to the opposite directions. Accordingly, it is better to assume a two-valued function in the vicinity of those values of the prospective charge. Such overvoltages are only realized under the condition that the dielectric strength between the contacts will withstand the transient recovery voltage. In a circuit breaker with the slower dielectric recovery strength, in spite of the distinguished ability of the current chopping, a reignition prevents the transient oscillation from building up and hence reaching to its higher crest. A circuit breaker with less successive reignitions may show a two-valued characteristic. Such a relation is evidently found in the breaker "Tamagawa D-2" and apparently in "Yokota D-3". It is not necessary to assume such a specific consideration in Fig. 3.12, where the summation of the prospective charges is taken over the three lines, because the large inrush currents flow in the other two lines before and after the zero passage of the current concerned as shown in Fig. 3.14 and also because the maximum overvoltage is plotted toward the right side of the diagram.

In the self-quenching type circuit breaker, for example, "Tamagawa D-4", many plotted points fall toward the right side corresponding to the large prospective charge. It may be difficult to quench even the small current just after the separation of the contacts, because the quenching energy of this type of breakers derived from the arc energy of the interruption is relatively small. So that, the final quenching action is apt to be realized at a next zero passage after the subsequent inrush period. Such relation produces less corresponding points in lower prospective charge. As shown in the investigation about the interruption of the small capacitive current, the above-mentioned tendency is supported by the fact that only the current approach to zero, not the actual zero passage, cannot be a chance to achieve a rupturing in a self-quenching circuit breaker.

The physical meaning, how the overvoltage due to the current chopping depends upon the prospective charge, may be considered as follows. The quenching performance of a circuit breaker is affected by the energy diverged from the arc. Some lapse of time will be needed for the air flow to grow up to the final condition owing to the compressibility of the air in the duct. Especially when the contacts begin to open during the higher current period, the current variation with time will give remarkable influences on the condition across the contacts. The air flow will be intercepted by the arc through which the large inrush current is carried. As soon as the current suppression is over, after a pretty long duration of time, the extreme strong air flow seems to pass through the contacts and to interrupt a remarkable current amount suddenly. And when the such suppression period will become shorter, the first impact of air flow and hence the instantaneous chopped current would seem to be reduced in magnitude. The

former corresponds to the case of the interruption with larger prospective charge, and the latter with smaller one.

§ 4. Analysed wave forms of three phase inrush current

When the alternating voltage is impressed on a single-phase or a three-phase unloaded transformer, excessive current may develop and its wave form may be far from a sinusoidal one. In the previous section, it is shown that overvoltages due to current chopping depend upon a time integration of prospective current that would continue to flow with the same form as before the separation of the contacts. Thus, it is possible to analyse the inrush current in order to estimate the frequency of occurrence of overvoltages theoretically. The reasons why the inrush current takes deformed wave forms are that at the instant of switching the magnetic flux will have the continuous magnitude as immediately before, and that the iron core has inherently a saturated magnetic characteristic. In case of a single phase transformer, the maximum current is observed when the circuit is closed at the vicinity of the zero passage of the feeding voltage, corresponding to 0° or 180° , and no inrush current at the vicinity of the voltage crest corresponding to feeding voltage reaches to the crest where the phase angle is 90° or 270° . On the contrary, a three-phase bank with isolated neutral always requires a quantity of inrush current after closing even if one of the lines is closed at the voltage crest.

The following calculation is carried out on the Y-connected bank with isolated neutral and open secondary windings, in which case three single-phase transformers are used in order to avoid the mutual interferences of the iron cores. It is the main purpose to find the amount of the time duration during which the inrush current is flowing, introducing the assumed magnetizing characteristic. As indicated in Fig. 3.15, the specific permeability μ of the core is so assumed as to hold a large value within the range below the flux level ϕ_s , and to fall down to unity in the range over that level. If the residual magnetism is left in the magnetic circuit, as will frequently occur in the actual transformers, it often magnifies the inrush peaks. Such a residual magnetism is mainly affected by the procedure of the previous interruption. To avoid the complexity, and to keep the theory not so far from the actual phenomena, the effect of the residual magnetism might be neglected, so that the initial flux will be assumed zero for the calculation. Other influences of source impedances, ohmic resistances and

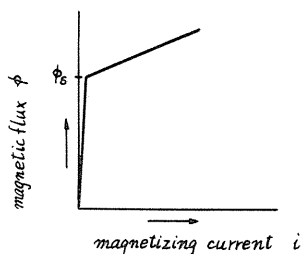


FIG. 3.15. Assumed magnetic characteristic.

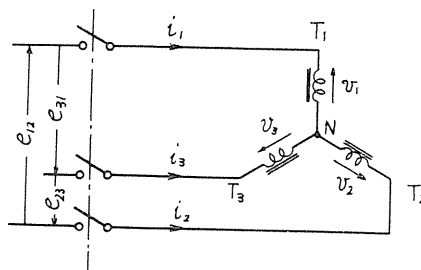


FIG. 3.16. Directions of voltages and currents.

losses in the transformers are also neglected, as they are able to be regarded as infinitesimals for the purpose. The assumed direction of voltage and current in every part of the circuit elements is shown in Fig. 3.16. The voltages across the windings, v_1 , v_2 and v_3 are not always kept equal to the phase voltages. Only the line-to-line voltages keep the balanced three-phase relation as follows.

$$\left. \begin{aligned} e_{12} &= v_1 - v_2, \\ e_{23} &= v_2 - v_3, \\ e_{31} &= v_3 - v_1. \end{aligned} \right\} \quad (1)$$

At the neutral point N in Fig. 3.16,

$$i_1 + i_2 + i_3 = 0 \quad (2)$$

is provided. The following equations are given

$$\left. \begin{aligned} n \frac{d\phi_1}{dt} &= v_1, \\ n \frac{d\phi_2}{dt} &= v_2, \\ n \frac{d\phi_3}{dt} &= v_3, \end{aligned} \right\} \quad (3)$$

where n is the number of turns of each transformer, and ϕ_1 , ϕ_2 and ϕ_3 are the magnetic fluxes in respective winding. In general, in a transformer bank with different inductances, Eq. (3) turns out to

$$\left. \begin{aligned} L_1 \frac{di_1}{dt} &= v_1, \\ L_2 \frac{di_2}{dt} &= v_2, \\ L_3 \frac{di_3}{dt} &= v_3. \end{aligned} \right\} \quad (4)$$

Combining Eqs. (1), (2) and (4),

$$\left. \begin{aligned} \frac{di_1}{dt} &= \frac{L_3 e_{12} - L_2 e_{31}}{L_1 L_2 + L_2 L_3 + L_3 L_1}, \\ \frac{di_2}{dt} &= \frac{L_1 e_{23} - L_3 e_{12}}{L_1 L_2 + L_2 L_3 + L_3 L_1}, \\ \frac{di_3}{dt} &= \frac{L_2 e_{31} - L_1 e_{23}}{L_1 L_2 + L_2 L_3 + L_3 L_1}, \end{aligned} \right\} \quad (5)$$

are obtained. The assumed magnetic characteristic as shown in Fig. 3.15 means that each winding, according to the inclination, has two values of inductances, which are given as

$$\left. \begin{aligned} n\phi &= Li & \phi \leq \phi_s, \\ n\phi &= L'i & \phi > \phi_s, \end{aligned} \right\} \quad (6)$$

where the flux level ϕ_s is regarded as the boundary for the inductances L and L' . Considering how many numbers of transformers are eventually in the state

of saturation after the energizing operation, Eq. (5) can be developed and solved.

The difference between the two inductances depends on the values of μ , the magnitude of which holds more than a few thousands for the unsaturated region and reduces to unity which is equal to the specific permeability of air. Accordingly, L is very much larger than L' in their values. The magnitude of the current in an unsaturated period is only a little fraction of that in a saturated period and a graphical representation of the two at the same time is rather difficult. Thus, assuming the magnitude of the current through L may be zero as a limiting value, the solutions are finally given by the following simple forms.

(i) Every transformer unsaturated.

$$\left. \begin{aligned} i_1 &= 0 \\ i_2 &= 0 \\ i_3 &= 0 \end{aligned} \right\} \quad (7.1) \quad \left. \begin{aligned} \phi_1 &= \frac{1}{n} \int e_1 dt + \phi_{10} \\ \phi_2 &= \frac{1}{n} \int e_2 dt + \phi_{20} \\ \phi_3 &= \frac{1}{n} \int e_3 dt + \phi_{30} \end{aligned} \right\} \quad (7.2)$$

(ii) One transformer saturated.

(ii-1) $L_1 = L'$, $L_2 = L_3 \rightarrow \infty$

$$\left. \begin{aligned} i_1 &= 0 \\ i_2 &= 0 \\ i_3 &= 0 \end{aligned} \right\} \quad (8.1) \quad \left. \begin{aligned} \phi_1 &= \phi_{10} \\ \phi_2 &= -\frac{1}{n} \int e_{12} dt + \phi_{20} \\ \phi_3 &= \frac{1}{n} \int e_{31} dt + \phi_{30} \end{aligned} \right\} \quad (8.2)$$

(ii-2) $L_2 = L'$, $L_1 = L_3 \rightarrow \infty$

$$\left. \begin{aligned} i_1 &= 0 \\ i_2 &= 0 \\ i_3 &= 0 \end{aligned} \right\} \quad (9.1) \quad \left. \begin{aligned} \phi_1 &= \frac{1}{n} \int e_{12} dt + \phi_{10} \\ \phi_2 &= \phi_{20} \\ \phi_3 &= -\frac{1}{n} \int e_{23} dt + \phi_{30} \end{aligned} \right\} \quad (9.2)$$

(ii-3) $L_3 = L'$, $L_1 = L_2 \rightarrow \infty$

$$\left. \begin{aligned} i_1 &= 0 \\ i_2 &= 0 \\ i_3 &= 0 \end{aligned} \right\} \quad (10.1) \quad \left. \begin{aligned} \phi_1 &= -\frac{1}{n} \int e_{31} dt + \phi_{10} \\ \phi_2 &= \frac{1}{n} \int e_{23} dt + \phi_{20} \\ \phi_3 &= \phi_{30} \end{aligned} \right\} \quad (10.2)$$

(iii) Two transformers saturated.

(iii-1) $L_1 = L_2 = L'$, $L_3 \rightarrow \infty$

$$\left. \begin{aligned} i_1 &= \frac{1}{2L'} \int e_{12} dt + i_{10} \\ i_2 &= -\frac{1}{2L'} \int e_{12} dt + i_{20} \\ i_3 &= 0 \end{aligned} \right\} \quad (11.1) \quad \left. \begin{aligned} \phi_1 &= \frac{1}{2n} \int e_{12} dt + \phi_{10} \\ \phi_2 &= -\frac{1}{2n} \int e_{12} dt + \phi_{20} \\ \phi_3 &= \frac{3}{2n} \int e_3 dt + \phi_{30} \end{aligned} \right\} \quad (11.2)$$

(iii-2) $L_1=L_3=L', L_2 \rightarrow \infty$

$$\left. \begin{aligned} i_1 &= -\frac{1}{2L'} \int e_{31} dt + i_{10} \\ i_2 &= 0 \\ i_3 &= \frac{1}{2L'} \int e_{31} dt + i_{30} \end{aligned} \right\} \quad (12.1)$$

$$\left. \begin{aligned} \phi_1 &= -\frac{1}{2n} \int e_{31} dt + \phi_{10} \\ \phi_2 &= \frac{3}{2n} \int e_3 dt + \phi_{20} \\ \phi_3 &= \frac{1}{2n} \int e_{31} dt + \phi_{30} \end{aligned} \right\} \quad (12.2)$$

(iii-3) $L_2=L_3=L', L_1 \rightarrow \infty$

$$\left. \begin{aligned} i_1 &= 0 \\ i_2 &= \frac{1}{2L'} \int e_{23} dt + i_{20} \\ i_3 &= -\frac{1}{2L'} \int e_{23} dt + i_{30} \end{aligned} \right\} \quad (13.1)$$

$$\left. \begin{aligned} \phi_1 &= \frac{3}{2n} \int e_1 dt + \phi_{10} \\ \phi_2 &= \frac{1}{2n} \int e_{23} dt + \phi_{20} \\ \phi_3 &= -\frac{1}{2n} \int e_{23} dt + \phi_{30} \end{aligned} \right\} \quad (13.2)$$

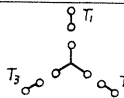
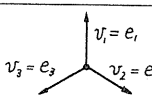
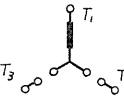
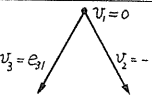
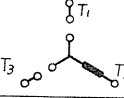
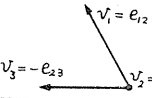
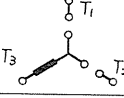
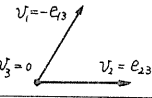
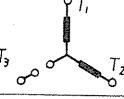
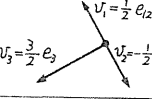
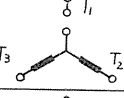
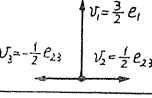
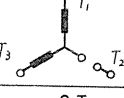
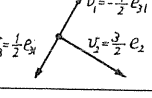
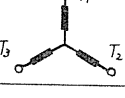
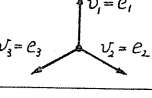
(iv) Every transformersaturated.

$$\left. \begin{aligned} i_1 &= \frac{1}{L'} \int e_1 dt + i_{10} \\ i_2 &= \frac{1}{L'} \int e_2 dt + i_{20} \\ i_3 &= \frac{1}{L'} \int e_3 dt + i_{30} \end{aligned} \right\} \quad (14.1)$$

$$\left. \begin{aligned} \phi_1 &= \frac{1}{n} \int e_1 dt + \phi_{10} \\ \phi_2 &= \frac{1}{n} \int e_2 dt + \phi_{20} \\ \phi_3 &= \frac{1}{n} \int e_3 dt + \phi_{30} \end{aligned} \right\} \quad (14.2)$$

According to the above-mentioned assumptions, an unsaturated transformer is equivalent to an open circuit. Table 3.1 shows the equivalent circuit and the vector diagram corresponding to every saturated condition. Since the actual magnitude of inrush peak depends on the structure, the rated voltage and the rated capacity of a transformer, the magnitude of $E/\omega L'$ is taken as a unit amount to express the value of inrush current, where E is the crest of the phase voltage, ω is 2π times the system frequency. Fig. 3.17 shows two examples of analysed inrush current, where $E/\omega L'$ is shown as 100%, each line is represented by phase a , b or c following the positive phase sequence, and the time, when a transformer is energized, is indicated by the electrical angle of the phase voltage in phase a , i.e. θ'_a . All sorts of the wave forms of the inrush currents actually realized in three lines under the arbitrary conditions can be typically represented by those when the phase angle θ'_a is restricted between 0° and 60° . Such relation is introduced in Table 3.2. Wave forms shown in Fig. 3.17 only correspond to the first period of the alternation just after the closing. Though the magnetic flux condition does not rigorously return back to the original state at the end of one period, 360° , the flux in transformer simultaneously passes through or approaches to zero at that time and nearly the same states are to be repeated successively in the following periods. These wave forms are quite analogous to the inrush current in the actual power systems. Indeed, such inrush is not sustained forever but gradually decays with the time by the effects of various losses, which are neglected in this analysis. It is rather difficult to estimate the various losses and also to determine the degree of the time decay quantitatively. Fig.

TABLE 3.1. Equivalent Circuits and Vector Diagrams
Corresponding to Every Saturated Condition

saturat- ed condition	$L_1 \quad L_2 \quad L_3$	Equivalent circuit	voltage vector
3 transf. un- saturat- ed	$\infty \quad \infty \quad \infty$		
1 transf. saturat- ed	$L' \quad \infty \quad \infty$		
2 transf. un- saturat- ed	$\infty \quad L' \quad \infty$		
	$\infty \quad \infty \quad L'$		
2 transf. saturat- ed	$L' \quad L' \quad \infty$		
1 transf. un- saturat- ed	$\infty \quad L' \quad L'$		
	$L' \quad \infty \quad L'$		
3 transf. saturat- ed	$L' \quad L' \quad L'$		

3.18 shows two characteristics of decaying of inrush current in the actual transformers. It can be seen that the inrush peaks decay to about 50 to 40% of the first peak after 20 cycles. Since a few seconds are required for the complete fading out of this asymmetrical component, the saturated versus unsaturated period in one cycle would not remarkably be changed within the first 20 cycles.

Now, the lower current period can be obtained from the analysed wave forms. The off-peak current ratio is plotted against the electrical angle of the phase when the switching is effected. The results are shown in Fig. 3.19. From this curve, the frequency of occurrence of the off-peak current ratio may be derived. In Fig. 3.19, the off-peak current ratio between a and b is realized by the closing procedure at the phase angle between a_1 and b_1, \dots, a_4 and b_4 , which are all projected regions of (a, b) on the curve. Accordingly, the frequency of occurrence of the region (a, b) is given by

$$\frac{(a_1, b_1) + (a_2, b_2) + (a_3, b_3) + (a_4, b_4)}{180^\circ} \times 100\%.$$

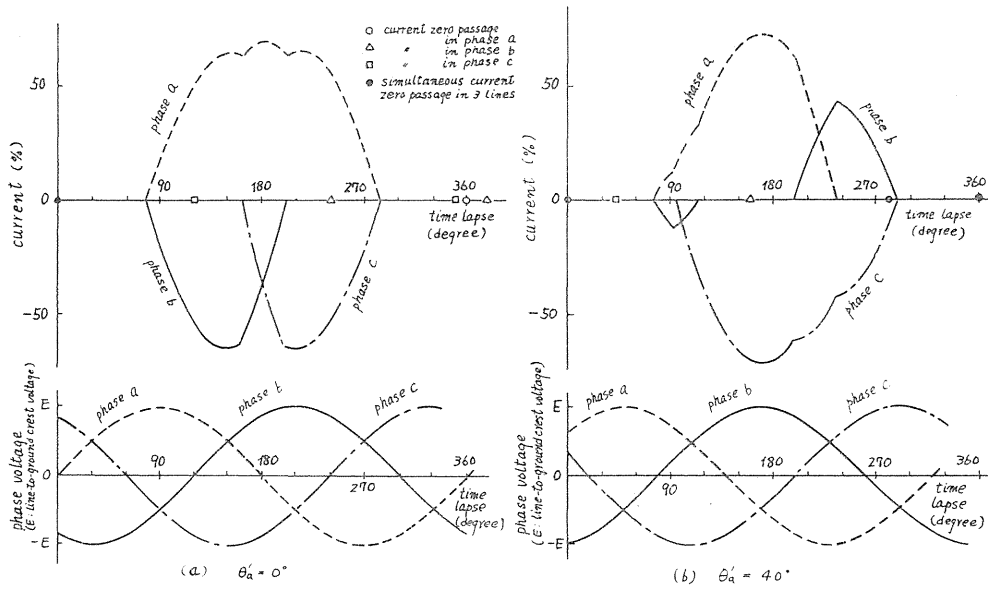


FIG. 3.17. Analysed inrush current forms of an unloaded three phase transformer.

TABLE 3.2. Relation Between the Inrush Current

Corresponds to this line for $0^\circ \leq \theta'_a < 60^\circ$ ↓	This lines → For this range of ↓	a	b	c
a	$0^\circ \leq \theta'_a < 60^\circ$			
b	$60^\circ \leq \theta'_a < 120^\circ$ inverse polarity		$0^\circ \leq \theta'_a < 60^\circ$	
c	$120^\circ \leq \theta'_a < 180^\circ$		$60^\circ \leq \theta'_a < 120^\circ$ inverse polarity	$0^\circ \leq \theta'_a < 60^\circ$
a			$120^\circ \leq \theta'_a < 180^\circ$	$60^\circ \leq \theta'_a < 120^\circ$ inverse polarity
b				$120^\circ \leq \theta'_a < 180^\circ$

The hystogram estimated with the step of every 5% is shown in Fig. 3.20. There are two maxima, one at 45% and the other at 65% of the off-peak current ratio, approximately. The fact will be likely to support the result of Fig. 3.8. The off-peak current ratio common in three lines lies between 40 and 44%. The experimental result of Fig. 3.8 shows that the above common ratio has the trend to take lower values and to concentrate around that value.

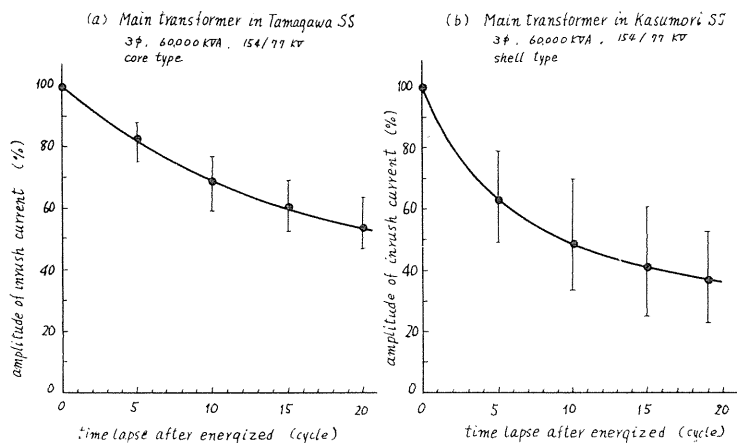


FIG. 3.18. Decrement of inrush magnetizing current of unloaded transformers in 60 c/s systems.

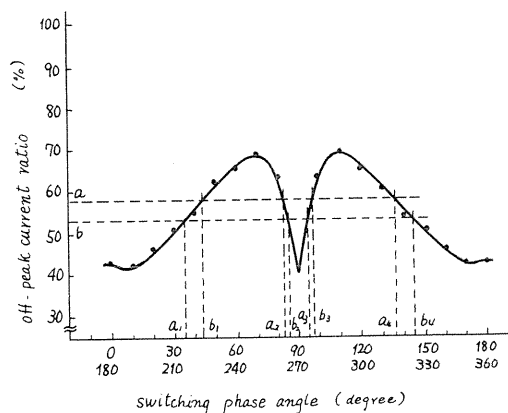


FIG. 3.19. Analysed off-peak current ratio.

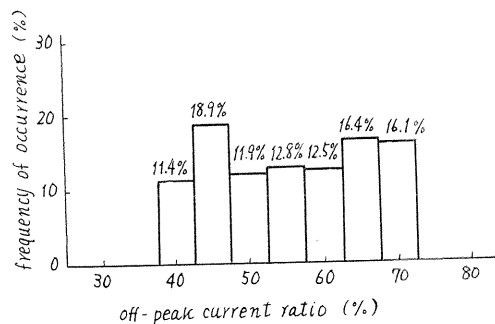


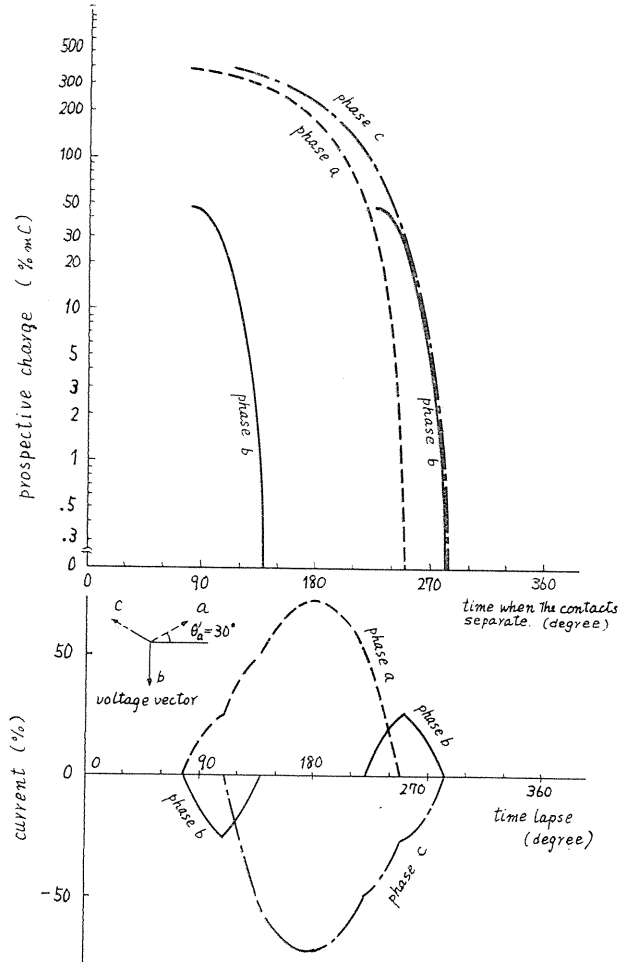
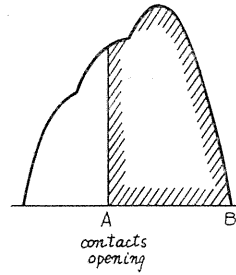
FIG. 3.20. Estimated frequency of occurrence of off-peak current ratio.

§ 5. Theoretical determination of possible overvoltage distribution

(5.1) Determination of prospective charge

The inrush current forms of a certain transformer are given uniquely, depending on the phase angle at which the transformer is energized. The time when the contacts begin to separate may be quite at random during the interrupting process. Thus, the frequency of occurrence for overvoltages due to current chopping may be estimated by using the wave forms analysed in the previous section. A prospective charge is no more than a shaded area between the points A and B indicated in Fig. 3.21, the former being the point at which the contacts separate and the latter at which the current comes back to zero. So far as taking the logarithm of the prospective charge, the relative value of the shaded area is only required. The magnitude of the current $E/\omega L$ is taken as 100% and the time lapse is measured in millisecond. Thus, the unit of the area

FIG. 3.21. Inrush current wave form.

FIG. 3.22. Prospective charge against the time when the contacts separate in case of switching at $\theta'_a = 30^\circ$.

is expressed as "% mC" (millicoulomb). With the unit thus defined, the upper diagram of Fig. 3.22 shows the curves of the prospective charge against the time when the contacts separate. The logarithmic scale is used for the ordinate. The positive phase rotation is the time sequence of *a-b-c* in its turn and the basic

phase is designated by phase a . The closing time is shown by θ'_a which is the angle of the phase voltage in phase a . The maximum prospective charge is realized when the contacts begin to separate just before the higher current period. These curves do not change the type but only displace upwards or downwards even if the various numerical results are directly plotted. The prospective charge is calculated as zero if the contacts separate during the lower current period.

(5.2) *Overvoltage estimation by the conception of prospective charge*

In Fig. 3.23, the curve L in the left part shows the relation between the overvoltage and the prospective charge. This is the experimental curve showing the average values of the measured points. The curve L' is the correction to the phase in which the switch is closed at the crest of the phase voltage. The curve M in the right part shows the relation between the prospective charge and the time when the contacts separate. These two curves, curve L and curve M , may be combined together taking the axis representing the prospective charge as common. An only difficulty is to find out the corresponding point on the both diagrams because of the undetermined magnitude of the prospective charge. The upper limit of the prospective charge can be found by the switching test. Such magnitude should correspond to the maximum of curve M obtained from the calculation for various closing angles. Therefore, these two points must coincide with each other. Curve L' can also be available in order to check up the above treatment. The prospective charge, which is estimated from the actual wave form of phase W in Fig. 3.3(b), must coincide with the corresponding value in the group of curve M . These two procedures establish the relation between curve L and curve M , even if a numerical magnitude of each current is not explicitly obtained.

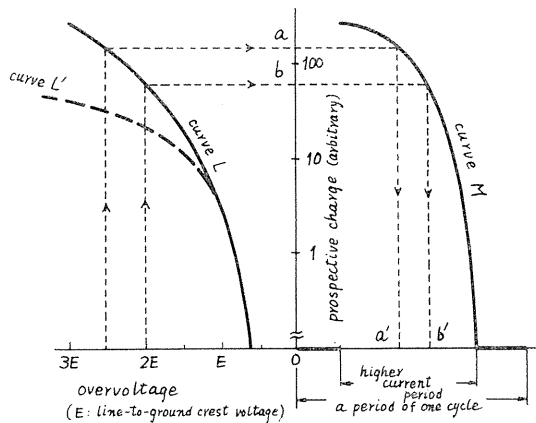


FIG. 3.23. Method of estimation of possible overvoltage.

In the left part of Fig. 3.23, a certain range of overvoltages, say between 2 and 2.5 times the normal crest, must be realized for the corresponding prospective charge between a and b , which can be obtained by the projection through curve L , tracing dotted lines in the direction of arrows. Next, in the right part of Fig. 3.23, this projected range (a , b) must be realized when the contacts begin to

separate at the time between a' and b' , which is derived by the projection through curve M as before. In other words, it may be considered that the overvoltages between 2 and 2.5 times the normal crest must occur when the contacts begin to separate between a' and b' , so that, the probability of the occurrence of overvoltages between this range is nothing but the ratio of the period (a' , b') to one cycle. Curve L' must be used for the extreme high transient overvoltage under the singular condition as shown in Fig. 3.14(a), but the ordinary curve L may be used under the condition as shown in Fig. 3.14(b). Since this difference depends on the chance when an abrupt rupturing is happened, it is quite difficult to point out that probability. As to the estimation of the final rupturing, one half of all the cases are assumed to be ruptured before zero passage and the other half after it.

(5.3) Results estimated

It had better to survey the switching abilities of each air-blast circuit breaker examined. Since the circuit breaker "Tamagawa D-2" is accompanied with few reignitions in an interrupting process, it may be considered as one of the most modern types of circuit breakers. In this respect, "Yokota D-3" follows the preceding and is succeeded by "Yamaguchi D-1" and "Kasumori D-5". Especially, "Kasumori D-5" shows a slower and irregular recovery of dielectric strength between the contacts during the quenching period.

The frequency of occurrence of overvoltages for each circuit breaker is estimated by the method described in the previous section. Two examples are shown in Figs. 3.24(a) and (b), in which the abscissa shows the closing angle of a phase voltage in degrees and the ordinate shows the frequency of occurrence of overvoltages in percent. These curves plotted are quite likely to be arranged symmetrically with respect to the vertical line of 90° . Fig. 3.24(b), in which the curve L' is considered, has a small maximum at the closing angle of 90° . This represents the fact that the possibility of the occurrence of the highest overvoltage will be expected when a circuit breaker interrupts and inrush current after energizing a transformer at that phase angle. On the contrary, in case of Fig. 3.24(a), no possibility of such overvoltages will be expected with the closing angle of 90° , because the reignitions between the contacts are apt to suppress the building up of a transient voltage. In case of "Yamaguchi D-1", the overvoltages more than 2.5 times the normal crest are expected in the very line where the closing angles happen to fall between -30° and $+30^\circ$, but in case of "Tamagawa D-2", such overvoltages are foreseen in almost all the lines except the cases of closing angles between 70° and 80° and between 100° and 110° . Thus, the highest overvoltage more than 2.5 times the normal crest may occur in the line where the position of the voltage vector at switching-on is within the shaded area in Fig. 3.25. If the three-phase balanced voltage vectors with the phase difference of 120° are put on those figures, only one of the three falls within the shaded area in case of "Yamaguchi D-1", but almost all of the three are contained in the shaded area in case of "Tamagawa D-2". In an interruption of the three-phase circuit, three values of phase angles must be considered at the same time. Since a great number of experiments result in the uniform distribution of closing phase angles, the resultant frequency of occurrence may be estimated by Fig. 3.24. Such results are shown in Figs. 3.26(a) to (e). In these figures, a solid

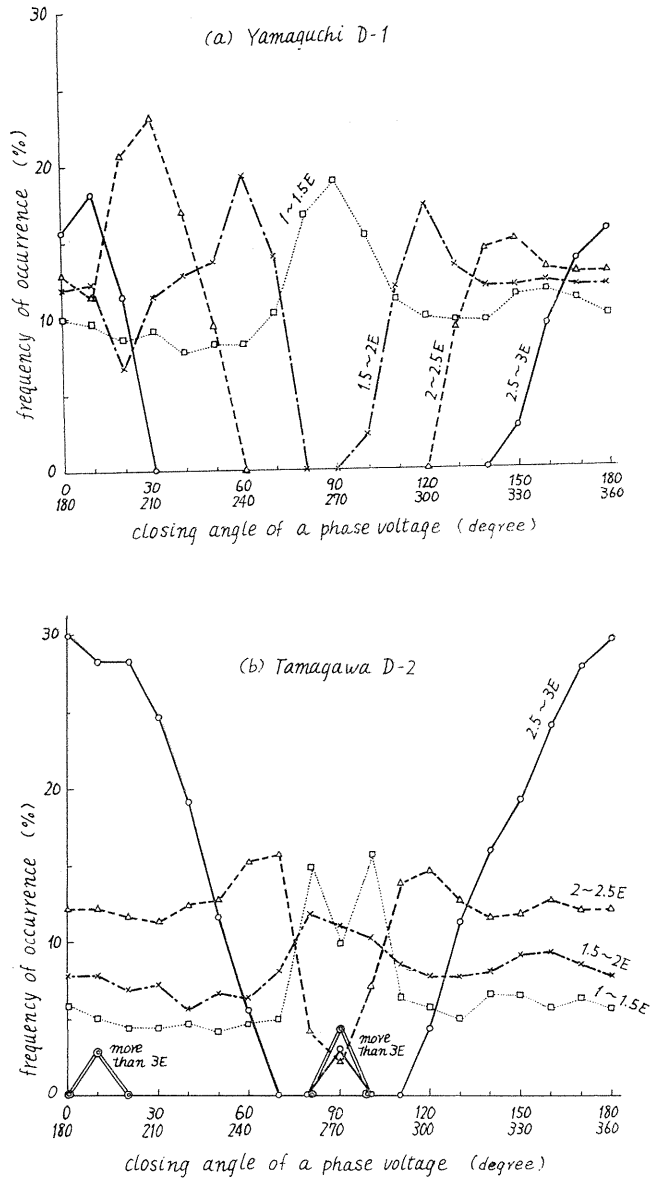


FIG. 3.24. Frequency of occurrence of overvoltages against the closing angle of a phase voltage.

line represents the estimated results and a dotted line the actual results obtained from the experiments shown in Table 1.1. The fact that both lines are closely drawn shows the good estimation of the theory. It is remarkable that the frequency of occurrence in "Tamagawa D-2" has a maximum at the intermediate level of 2 to 3 times the normal crest.

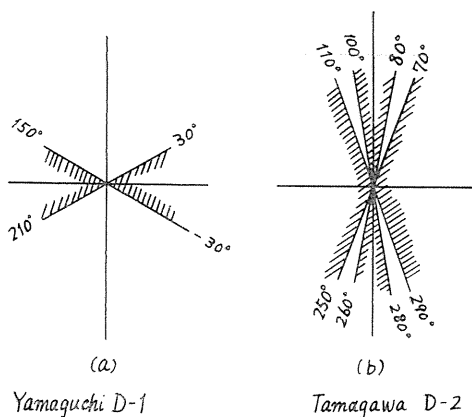


FIG. 3.25. Ranges of closing angle for overvoltages of $2.5E$ and more (shaded area).

(5.4) Supplementary notes

One of the reasons for the differences between dotted lines and solid ones is the fact that the characteristic L or L' is represented by a single curved line tracing the average values. Such difference is remarkable for the lowest level. For example, in case of "Tamagawa D-2", the curve L starts from 0.8 times the normal crest as the average covering the values between 0.4 and 1.2 as shown in Fig. 3.11(d). So that, the resultant transient crest value in the lower current period is always treated as less than unity. On the contrary, in case of "Yokota D-3", since the curve L starts from 1.1, the resultant value in the lower current period, is estimated between the level of 1 to 2. This leads to the remarkable differences in the lowest level and the condition is more or less the same for the higher levels.

The common tendency in Fig. 3.26 is that the calculated frequency is always larger than the actual one for the lowest level of overvoltages in each circuit breaker. A reason for this difference is that the shaded period of (a, b) and (c, d) in Fig. 3.27 is regarded as the lower current period in this estimation. It may be rather difficult, however, to achieve the final rupturing when the contacts separate in the period (a, b), during which the actual inrush current is going to build up and the

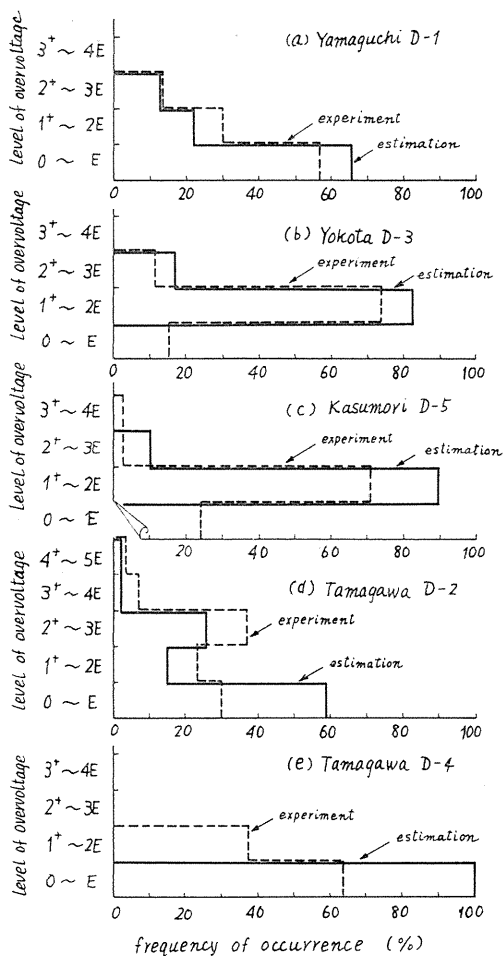


FIG. 3.26. Frequency of occurrence of overvoltages.

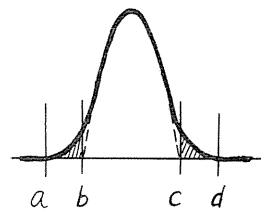


FIG. 3.27.

quenching action is almost invalid. Thus, it may be reasonable to consider that the final rupturing is put off until the following inrush is over. Therefore, it had better to regard the period (a, b) to be included in the higher current period, and better to expand the higher current period by 20° to 30° in electrical angles at least, and hence, the frequency of occurrence of the lowest transient peak will decrease by 5 to 8%. Since such practical expansion of the higher current period is equivalent to the extension of the left edge of curve M in Fig. 3.23, the frequency of occurrence in higher level of overvoltages also increases by the same rate.

A circuit breaker with slower recovery characteristic of dielectric strength generally prevents a transient oscillation from building up by a reignition between the contacts and a remarkable overvoltage is not recognized. Therefore, although the curve L' is regarded as the source of the highest overvoltage, it must be introduced according to the switching ability of the circuit breakers under consideration.

Chapter 4. A Few Comments on Switching Surges

§ 1. Standard surges for testing insulations

The characteristics of switching surges in actual power systems are not still now fully investigated in details, for example, in their magnitudes as well as in their wave forms. The dielectric strength of materials for switching surges must be discussed in relation to the actual system performances. Such problems are treated hereafter by using the results of the analyses in Chapter 2. The quoted three conditions are as follows: the circuit condition of type B, the five interrupting processes assorted and the case of the first reignition after the temporary interruption of three phase currents. The curves tracing the first crests of transient voltages, shown in Figs. 2.15, 2.18 and 2.21, indicate the possible highest overvoltages for every reignited time. Therefore, the resultant highest line-to-ground overvoltages regardless of the five processes are summarized: in Fig. 4.1 for an initial reignition, in Fig. 4.2 for a reignition over two lines and in Fig. 4.3 for a reignition over three lines. The highest line-to-line overvoltages during a two or three phase reignition are shown in Fig. 4.4. The ordinate shows the absolute values of overvoltages in times the crest of the phase voltage just before a reignition, and the abscissa the time lapse after the temporary interruption in electrical angle. The thick line indicates the limit of overvoltages for the interrupting process in the series of $\theta'_a = 90^\circ$ and $\omega t_0 = 0^\circ$ to 90° , and the fine line for $\theta'_a = 60^\circ$ and $\omega t_0 = 0^\circ$. Figs. 4.2 and 4.3 show that the maximum overvoltage due to a two or three phase reignition is always less than 3 times the normal crest of the phase voltage just before a reignition. The oscillating frequency generally takes several hundreds of cycles. The most troublesome problem for the estimation of an actual overvoltage is how to take the basic crest of the phase voltage. The phase voltage may take various amounts in power systems according to the time and location. Thus, $1/\sqrt{3}$ times the nominal line-to-line voltage is taken as the reference. Since the highest system voltage may be allowable up to 120% of the nominal voltage, the limit of overvoltage must be considered as 3.6 times ($=3 \times 1.2$). From the view-point of the insulation, an adequate quantity of tolerance must be left, say 20%, in order to keep the normal operation of the

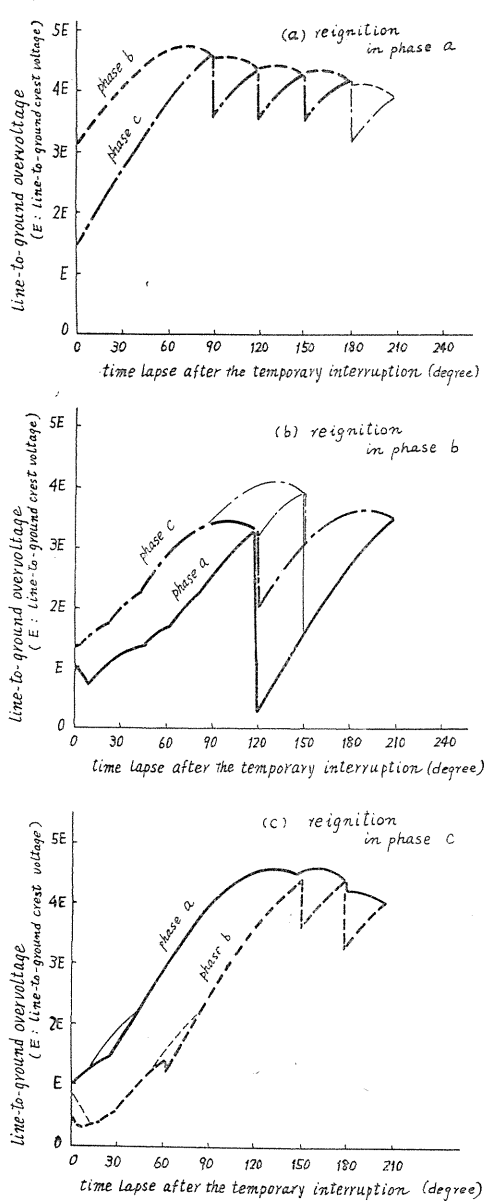


FIG. 4.1. Resultant highest line-to-ground overvoltages for an initial reignition.

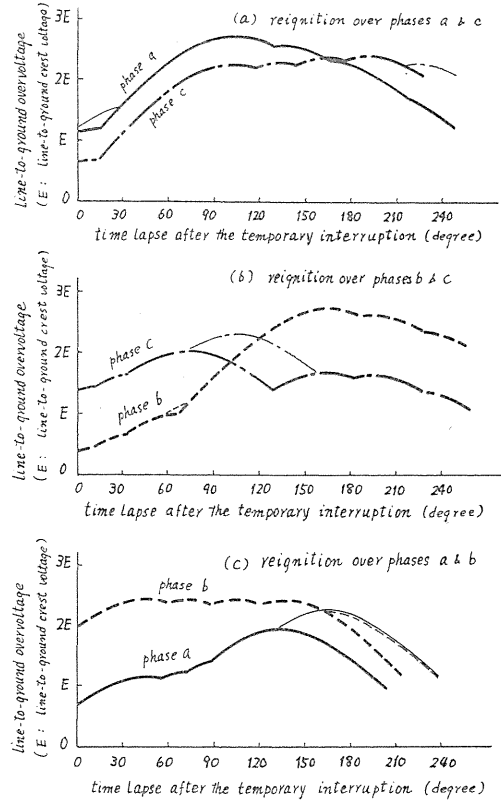


FIG. 4.2. Resultant highest line-to-ground overvoltages for a reignition over two lines.

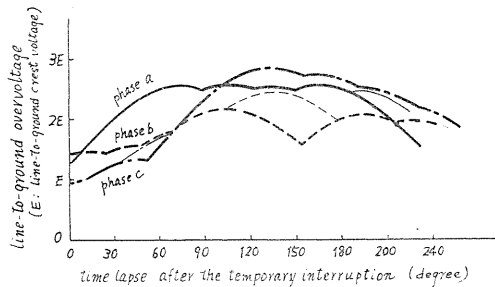


FIG. 4.3. Resultant highest line-to-ground overvoltages for a reignition over three lines.

systems. Thus, the insulation must withstand 4.5 times ($=3.6/0.8$) at least. The original value, 3 times the normal crest, is derived by using the average damping factor obtained from Fig. 2.8 with respect to 400 c/s as an example. Fig. 2.8 indicates that the free oscillation with 400 c/s attenuates to 70% of the initial amplitude in course of its half cycle. Thus, if some safety factor for the damp-

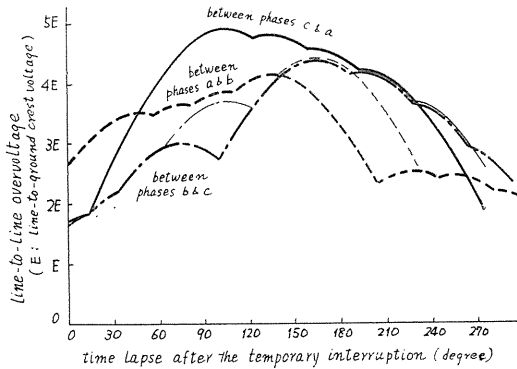


FIG. 4.4. Resultant highest line-to-line overvoltages for a reignition over two or three lines.

It had better, in this case, to provide another method of suppressing overvoltages rather than to afford an ample dielectric strength for all insulations so as to withstand such a high overvoltage, because this value is far from the conception of the actual insulation strength. This transient voltage appears across the small capacitance C_s on the bus side as shown in Fig. 2.14 and the electrostatic energy contained may be rather small. Thus, it will be more economical to absorb the transient peak by means of a lightning arrester if possible. If such a method is applicable it is only sufficient to reproduce the first crest of the free oscillation during a reignition over two or three lines as a testing wave forms against switching phenomena, the frequency of which must be several hundreds of cycles and the crest 5 times the crest of the nominal phase voltage.

§ 2. Tolerable reignition of circuit breakers

In the former section an upper limit of strength required for the insulation is discussed under the condition that a reignition may be caused at any time in a circuit breaker, but this limit may be reduced, if a reignition is confined in some restricted time intervals. Table 4.1 shows the maximum time lapse to a reignition from the temporary interruption allowing the overvoltages below two times the crest for various cases. This requires the insulation strength to withstand at least 3.5 times. And, therefore, assuming the overvoltage of 2 times as a boundary, two or three phase reignitions may be classified into two groups; one is a reignition and the other a restriking, according to a narrow sense of ordinary classification. The condition scarcely holds in the case of the initial reignition. For a reignition on phase *b* in Table 4.1 after the time lapse of 32° (less than 90°) from the previous quenching easily induces the transient crest as high as 2 times. This is also the reason why it is reasonable to design a circuit breaker so as to be able to absorb the overvoltages derived from the initial reignition by proper limiting devices.

ing of free oscillation is estimated, say 10%, the dielectric strength is required up to 5 times ($=4.5/0.9$) the crest of the nominal phase voltage.

Fig. 4.1 indicates that the maximum overvoltage due to an initial reignition may reach to 5 times the crest of the phase voltage just before a reignition, if the first crest of its transient is realized. This time there may be obtained an overvoltage of 8.3 times ($=5 \times 1.2/0.8 \times 0.9$) the nominal phase voltage by the same procedure. The oscillating frequency generally takes several thousands of cycles, as the oscillatory circuit is independent of the line capacitances.

TABLE 4.1. The Condition with Overvoltages Nearly no more than $2E$
(for the series of $\theta'_a=90$)

Reignition type	Reignited phase	For phase	Time lapse after the temporary interruption (degree)
initial reignition	a	b	0
		c	0
	b	c	32
		a	71
	c	a	32
		b	74
2-phase reignition	$a-c$	a	46
		c	70
	$c-b$	c	63
		b	107
	$b-a$	b	— (slightly over $2E$)
		a	— (not over $2E$)
3-phase reignition	—	a	30
		b	80
		c	76

§ 3. Overvoltages amended by circuit breaker characteristics

The careful observations of the quenching process will lead to the rigorous estimation of possible overvoltages. Various experimental results present no detailed information about the physical condition between the contacts of circuit breakers in actual power systems. More informations should be acquired from the actual oscillograms observed. The following results can be obtained on the frequency of occurrence of overvoltages due to the interruption of inrush magnetizing current of unloaded transformers. According to the consideration in Chapter 3, the possible overvoltages are estimated according to the manner how the curve L (the relation between the overvoltage and the prospective charge) is associated with the curve M (the relation between the opening chance and the prospective charge). In brief, the rupturing performance, with respect to the switching overvoltages, should be considered from the view-points of the ability of current chopping and the recovery rate of the dielectric strength between the contacts. The improved ability of current chopping seems to be realized more easily than the high recovery rate of dielectric strength in air-blast circuit breakers. Indeed, the early types of air-blast circuit breakers interrupted the magnetizing current with many successive reignitions, while more recent breakers are accompanied with few reignitions. This fact supports the above-mentioned deduction being the truth. Since the steep transient oscillation will build up to the extreme crest in a breaker with the excellent rupturing performance, the maximum of the curve L may reach up to 3 times the crest. Thus, the higher part of the curve M is occupied by the higher voltage level, say 2 to 3 times, and the resultant distribution of overvoltages has a maximum at that level. Next, in a circuit breaker with the improved ability of current chopping and the slower recovery rate of dielectric strength, a reignition prevents the transient oscillation from arriving at the extreme crest and the maximum of the curve L

will only reach to 2.5 times. Thus, the above-mentioned maximum displaces downward to the lower level of overvoltages. Moreover, in a circuit breaker without any ability of current chopping, the curve L is independent of the prospective charge and shows the flat characteristics, and, therefore, no remarkable overvoltage is expected. The overvoltages more than 3 times may be realized in the breaker with the most excellent rupturing performance, especially in case of a singular inrush current.

Conclusion

In case of the interruption of line charging current at the terminals of a transformer with an isolated neutral, which is designated by the circuit condition of type B in the treatise, the following are the conclusions.

(1) The first extinction in three line currents is achieved in the neighbourhood of the crest of the phase voltage, which coincides with the traditional concept.

(2) The period between the first rupturing and the second of the current is certainly shorter than 90° , and scatters between 0° and 90° . This fact is quite different from the traditional concept.

(3) Five patterns are presented to explain interruption processes and switching overvoltages.

(4) As the result of careful examination of oscillograms taken in actual power systems, reignitions are more frequently induced between the contacts in second ruptured lines. And the analysis shows that the increasing rate of recovery voltages in these lines are higher than that in the first one.

(5) It is analytically estimated that most of the initial reignitions after a temporary clearing in three lines develop into the two or three phase reignitions at the same rate and about 8% of initial ones remain undeveloped.

(6) The damping time constants of free oscillations, in actual power systems, due to the reignition are empirically expressed as the inverse proportion of 0.9 power of those frequencies.

(7) The time duration of a transient oscillation due to the reignition seems to have some relations with the cleared-up time prior to that reignition. The longer the cleared-up time is, the same is the duration.

(8) The so-called cumulative overvoltage scarcely seems to occur in actual systems and the case is estimated to be less than the rate of 0.003.

(9) With respect to each type of the first reignition caused just after the temporary interruption of three line currents, the limiting value of the first crest may be theoretically calculated as the function of the time when it is caused. The degree of overvoltages cannot be directly defined in an uneffectively grounded system by the simple expressions as are called reignitions or restriking.

(10) There may be two types of transient overvoltages due to a reignition: one is the oscillation induced by the initial reignition at the cleared-up terminals of the transformer and has the magnitude of 5 times as high as the normal crest and the frequency of several kilocycles, the other is that induced in the reignited lines and of 3 times as high and of several hundreds of cycles.

(11) The dielectric strength of various apparatus in power systems should be requested to withstand the switching surges of 5 to 8 times the nominal crest, which are the reasonably selected values in consideration of the highest allowable

system voltage, of the tolerance of dielectric strength and of the safety factors for damping.

(12) From the technical point of view, it is rather preferable to absorb the higher overvoltages by means of proper devices such as lightening arresters.

(13) A circuit breaker with no reignition or, at least, one within 90° tends to reduce the transient overvoltages to less than 2 times which, in turn, correspond to the severity of insulation of 3.5 times.

In case of interruption of inrush magnetizing current of an unloaded transformer with an isolated neutral, the conclusions are as follows:

(1) It is evident that the current chopping in this case is a vital cause of overvoltages, but various sorts of overvoltages are still caused under the same external conditions.

(2) It is experimentally concluded that the overvoltages due to current chopping depend exclusively on the prospective charge, which is defined by the integration of the current over the period between the time of opening of the contacts and the next current zero passage, assuming that the current keeps the same form as that of preceding loop.

(3) The magnetizing inrush current is theoretically estimated assuming that the magnetic characteristic of the transformer as represented by two straight lines.

(4) The results of the theoretical estimation of the frequency of occurrence for each rank of overvoltage are as following.

(i) The frequency of occurrence of higher overvoltages decreases simply in case of circuit breakers with moderate abilities.

(ii) That frequency of a moderate overvoltage has a remarkable maximum value in case of breakers with rather excellent abilities.

(iii) The highest overvoltage is caused only in most excellent breakers, accompanied with the singular inrush wave form.

(5) Though the numerical amount of the highest overvoltage depends on each circuit breaker, the frequency of occurrence of overvoltages always indicates the above-mentioned tendency according its abilities.

Acknowledgement

The author wishes to express his thanks to Professor Dr. I. Miyachi of Nagoya University for his personal instructions and valuable advices during the last seven-years period. The author also expresses his appreciation to Professor Dr. U. Shinohara and Professor Dr. K. Yamamoto of Nagoya University, respectively, for their valuable discussions and encouragements. He is also grateful to the staffs and the students in Faculty of Engineering, Nagoya University, for their hearty assistances in some experiments and analyses.

References

- 1) H. Baatz: Überspannungen in Energieversorgungsnetzen (Book) 1956, p. 255.
- 2) J. Slepian: Extinction of an AC Arc, *TAIEE* **47** (1928), p. 1398-1408.
- 3) L. F. Hunt and o.: Switching Overvoltage Hazard Eliminated in High-Voltage Oil Circuit Breakers, *TAIEE*, **62** (Feb. 1943), p. 98-106.
- 4) R. Rüdenberg: Transient Performance of Electric Power Systems (Book), 1950, p. 588.
- 5) H. L. Byrd and o.: A Three-Cycle 3,500 MVA Air-Blast Circuit Breaker for 138,000 V

- Service, TAIEE, **64** (May 1945), p. 229-32.
- 6) for ex. R. Thaler: Synthetic Testing Method of High Voltage Circuit Breakers for Switching Capacitors and Lines, CIGRE, 1960, No. 116.
 - 7) L. V. Bewley: Traveling Waves on Transmission Systems (Book), 1951.
 - 8) H. A. Peterson: Transients in Power Systems (Book), 1951, p. 128.
 - 9) for ex. L. V. Bewley: Equivalent Circuits of Transformers and Reactors to Switching Surges, TAIEE, **58** (1939), p.797-802.
 - 10) T. H. Lee: The Effect of Current Chopping in Circuit Breakers on Networks and Transformers I—Theoretical Considerations, TAIEE (Aug. 1960), p. 535-44.
 - 11) Restriking Voltage Committee: Restriking Voltage in Power Systems, *Denki kyodô-kenkyû*, **14**, 2 (Apr. 1958).
 - 12) H. Mizutani: On the Problem of Interruption of Charging Current, *Fuji-jihô*, **28**, 2, 4, 5, 6 (1955).
 - 13) R. D. Evans and o.: System Recovery Voltage Determination by Analytical and AC Calculating Board Methods, TAIEE, **56** (Jun. 1937), p. 695-703.
 - 14) E. L. Harder: A Large Scale General-Purpose Electric Analog Computer, TAIEE, **67** (1948), p. 664-73,
 - 15) I. B. Johnson and o.: Switching Surge Voltages in High-Voltage Stations, TAIEE (Feb. 1954), p. 69-79.
 - 16) I. B. Johnson and o.: Some Fundamentals on Capacitance Switching, TAIEE (Aug. 1955), p. 727-36.
 - 17) R. D. Evans and o.: Power-System Transients Caused by Switching and Faults, TAIEE, **58** (Aug. 1939), p. 386-96.
 - 18) for ex. A. F. Darland: Interrupting Capacity Verification of 10,000 MVA 230 kV Oil Circuit Breakers for Grand Coulee Power Plant, TAIEE, **70** (1951), p. 1386-97.
 - 19) L. R. Bergström: The Field Testing of 220 kV Air Blast Circuit Breaker, EE (Feb. 1951), p. 118-24.
 - 20) G. Jancke: The Field Testing of 380 kV Circuit Breakers, CIGRE, 1954, No. 106.
 - 21) 22) p. 71.
 - 22) A. Greenwood: The Effect of Current Chopping in Circuit Breakers on Networks and Transformers II—Experimental Techniques and Investigations, TAIEE (Aug. 1960) p. 545-55.
 - 23) H. Kindler: Modelversuche zum Abschalten Leerlaufen Transformatoren, ETZ-A, **81**, 1 (1960), p. 7-11.
 - 24) E. W. Boehne: The Geometry of Arc Interruption, TAIEE **60** (1941), p. 524-32.
 - 25) *ibid.*, **63** (1944), p. 375-86.
 - 26) A. F. B. Young: Some Researches on Current Chopping in High Voltage Circuit Breakers, PIEEE, **100**, pt II, 76 (Aug. 1953), p. 337-53.
 - 27) R. Gert and o.: Contribution to the Study of Overvoltages' Results Obtained in Czecho-Slovak Systems, CIGRE, 1958, No. 336.
 - 28) C. H. Flurscheim: Factors Influencing the Design of High-Voltage Air-Blast Circuit Breakers, PIEEE, **96**, Pt II (1949), p. 557-85.
 - 29) S. Yamasaki: The Application of Non-linear Resistors to the Resistance-Switching, JIEE of Japan, **73**, 783 (1953), p. 1350-58.
 - 30) N. Nakanishi and o.: Fundamental Studies on the Suppression of Overvoltages with Non-linear Shunt Resistors at the Interruption of Small Inductive Currents, JIEE of Japan, **75**, 806 (1955), p. 1354-60.
 - 31) for ex. Y. Moriwaki: Calculation Method on Transient Phenomena (Katogenshō-keisan-ho), (Book), 1950, p. 89.
 - 32) F. Andé: Betrieb u. Anwendung von Leistungs- u. Regel Transformatoren (Book), 1954, p. 209.
 - 33) R. Buch und o.: Über Transformatoren mit annäherend sinusförmigen Magnetisierungsstrom, ETZ-B, **56**, 34 (Aug. 1935), p. 933-36.

- 34) J. Biermanns: Fortschritte im Transformatorenbau, ETZ B, **58**, 23 (Jun. 1937), p. 622-26.
- 35) for ex. M. Vidmar: Die Transformatoren (Book), 1921, p. 32-41.
- 36) for ex. 22) p. 630-41.
- 37) W. Schmidt: Vergleich der Größtwerte des Kurzschluß- u. Einschaltstromes von Einphasentransformatoren, ETZ-A, **79**, 21 (Nov. 1958), p. 801-6.
- 38) T. R. Specht: Transformer Magnetizing Inrush Current, TAIEE, **70** (1951), p. 323-28.
- 39) L. F. Blume and o.: Transformer Magnetizing Inrush Currents and Influence on System Operation, TAIEE, **63** (1944), p. 366-75.
- 40) AIEE Committee Report: Report on Transformer Magnetizing Current and Its Effect on Relaying and Air Switch Operation, TAIEE, **70** (1951), p. 1733-40.